

Plate convergence measured by GPS across the Sundaland/Philippine Sea Plate deformed boundary: the Philippines and eastern Indonesia

C. Rangin,¹ X. Le Pichon,² S. Mazzotti,¹ M. Pubellier,¹ N. Chamot-Rooke,¹
M. Aurelio,³ Andrea Walpersdorf¹ and R. Quebral³

¹Laboratoire de Géologie, Ecole Normale Supérieure, CNRS, UMR 8538, 24 rue Lhomond, 75231, Paris, France

²Collège de France, 6 place M. Borthelot, 75005, Paris, France

³Bureau of Mines and Geosciences, Quezon City, Metro Manila, Philippines

Accepted 1999 June 6. Received 1998 December 12; in original form 1998 January 4

SUMMARY

The western boundary of the Philippine Sea (PH) Plate in the Philippines and eastern Indonesia corresponds to a wide deformation zone that includes the stretched continental margin of Sundaland, the Philippine Mobile Belt (PMB), extending from Luzon to the Molucca Sea, and a mosaic of continental blocks around the PH/Australia/Sunda triple junction. The GPS GEODYSSSEA data are used to decipher the present kinematics of this complex area. In the Philippines, the overall scheme is quite simple: two opposing rotations on either side of the left-lateral Philippine Fault, clockwise to the southwest and counterclockwise to the northeast, transfer 55 per cent of the PH/Sundaland convergence from the Manila Trench to the northwest to the Philippine Trench to the southeast. Further south, 80 per cent of the PH/Sunda convergence is absorbed in the double subduction system of the Molucca Sea and less than 20 per cent along both continental margins of northern Borneo. Finally, within the triple junction area between the Sundaland, PH and Australia plates, from Sulawesi to Irian Jaya, preferential subduction of the Celebes Sea induces clockwise rotation of the Sulu block, which is escaping toward the diminishing Celebes Sea oceanic space from the eastward-advancing PH Plate. To the south, we identify an undeformed Banda block that rotates counterclockwise with respect to Australia and clockwise with respect to Sundaland. The kinematics of this block can be defined and enable us to compute the rates of southward subduction of the Banda block within the Flores Trench and of eastward convergence of the Makassar Straits with the Banda block. The analysis made in this paper confirms that this deformation is compatible with the eastward motion of Sundaland with respect to Eurasia determined by the GEODYSSSEA programme but is not compatible with the assumption that Sundaland belongs to Eurasia, as was often assumed prior to this study.

Key words: crustal deformation, fault motion, geodynamics, Global Positioning System (GPS), Indonesia, Philippines.

1 INTRODUCTION

Much of the active deformation of Southeast Asia results from its convergence with the relatively northward-moving Australia (AU) continental plate and with the westward-moving Philippine Sea (PH)/Caroline/Pacific oceanic plates (Fig. 1). Various marginal basins, trapped within this convergent triple plate junction, are presently consumed by active subduction zones. These include the West Philippine Basin, the oldest marginal basin of the PH Plate, and the Molucca, South China, Celebes and Sulu seas. These convergent plate

boundaries and their associated strike-slip fault zones delineate a wide active seismotectonic zone corresponding to the Philippine Mobile Belt (PMB) to the north and the triple junction area to the south. The discussion of the kinematic pattern within this zone, using the GEODYSSSEA combined GPS solution (Wilson *et al.* 1998), is the subject of this paper. This solution is mapped within the ITRF 1994 framework. A later solution within the ITRF 1996 framework fits the first solution within 3σ error ellipses (Simons *et al.* 1999). The eastward component is decreased by 3 mm yr^{-1} and the northward component increased by 3 mm yr^{-1} with respect to the solution used in

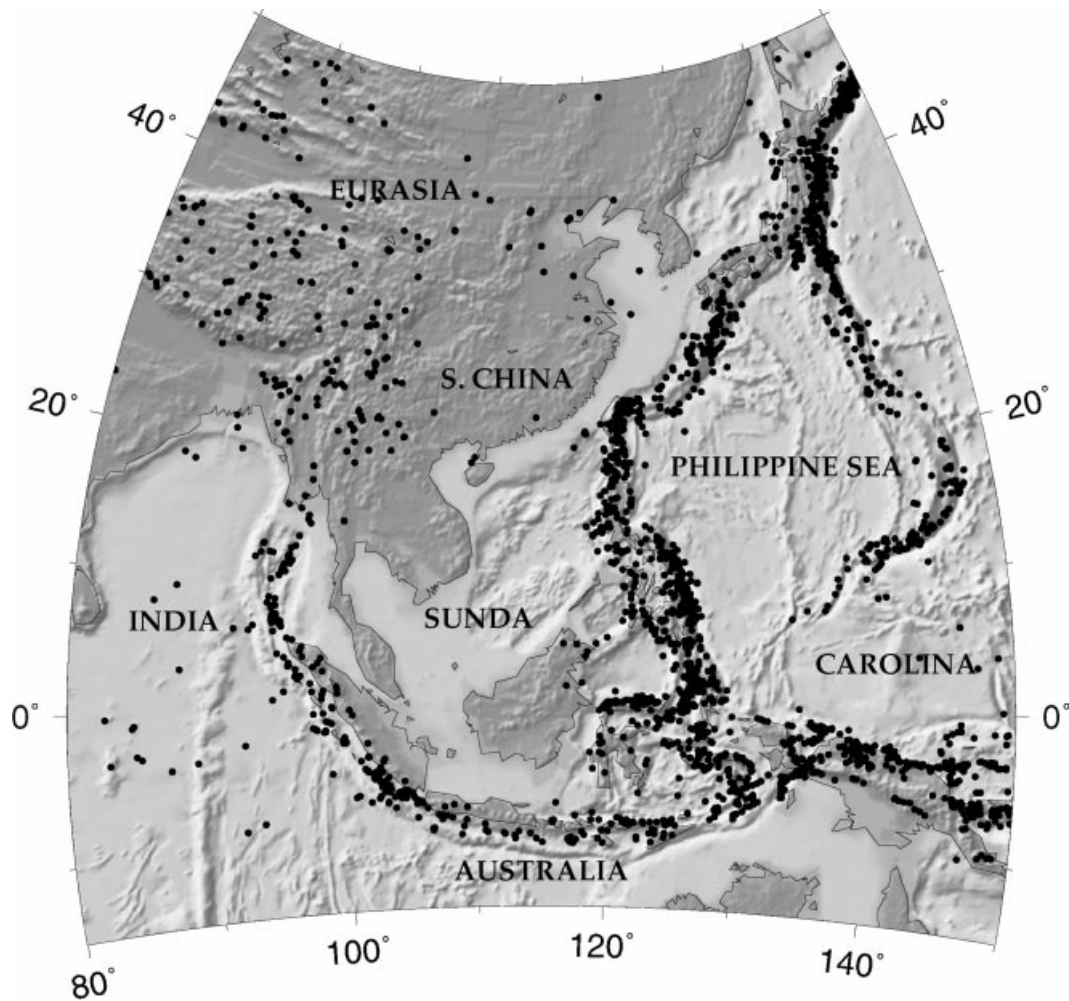


Figure 1. Locations of shallow earthquakes outlining the main plate boundaries. Note the 500 km wide active tectonic belt across the Philippine archipelago and Sulawesi. Note also the active seismicity along the Sulu archipelago and the discrete seismicity extending from the Red River Fault in Yunnan to Hainan and Taiwan.

this paper. These variations are within the uncertainties of the global solution. Table 1 lists the vectors derived from this solution in a Sundaland (SU) frame and Figs 2, 3 and 4 present the vectors within the SU, PH and AU reference frames, respectively. These reference frames are defined in Sections 2 and 3. In this paper, unless otherwise indicated, the frame of reference is the SU frame.

The GEODYSSSEA solution, based on data from two GPS measurement campaigns in December 1994 and April 1996, has been established by merging the results computed independently by four international data processing centres. The velocity field was obtained by combining the merged solutions for 1994 and 1996, with a formal error of $2\text{--}3\text{ mm yr}^{-1}$ for horizontal displacement rates and about 5 mm yr^{-1} for vertical motions. Chamot-Rooke *et al.* (1997, 1999) have shown that the relative precision within the network is equivalent to the formal errors. This good precision results from a careful measurement strategy (Wilson *et al.* 1998). It gives us the possibility of evaluating the relative motions along the main tectonic boundaries with a probable precision of 5 mm yr^{-1} or less when the results are directly derived from adjacent measurements.

In the following, we define the limit between the undeformed Sundaland block (SU) to the west and the deformed belt to the east. We then discuss the implications of the newly found kinematics of SU on the motions of SU with respect to AU and PH that are absorbed within this mobile belt. We next describe the tectonic set-up of the PMB and identify the main active faults and trenches that delineate the major blocks used to establish the kinematic pattern on the basis of the GEODYSSSEA vectors. After having analysed the GEODYSSSEA vectors within this belt to evaluate and correct for the possible effects of transient coseismic and interseismic phenomena, we proceed to a quantitative estimation of the motion absorbed within the main trenches and faults, starting from the east. This enables us to establish a simple model of the pattern of transfer of PH motion, from the Manila Trench to the NW to the Philippine Trench to the SW, mostly through rotation and strike-slip faulting. In the last section, we consider the deformation around the complex triple-point junction area around Sulawesi and north of Australia and identify an undeformed Banda block. Its established kinematics enable us to propose for the first time quantitative estimates of the motion on the Flores Trench and Makassar convergent zone.

Table 1. GEODYSSSEA GPS vectors with respect to Sundaland.

SITE	Latitude	Longitude	V (mm yr ⁻¹)	Azimuth (°)
BAKO	-6.49	106.85	1.53	252.29
KIT3	39.13	66.89	30.75	223.48
MALI	-2.59	120.90	26.25	294.35
TERN	0.86	127.34	98.95	289.50
TIDB	-35.40	148.98	78.63	5.01
TSKB	36.11	140.09	47.67	280.59
YARI	-29.05	115.35	68.46	20.55
COCO	-12.19	96.83	55.59	24.72
KARR	-20.98	117.10	72.10	13.56
MEDA	3.55	98.64	5.36	20.39
BENG	-3.79	102.25	25.36	339.21
CAMP	21.00	107.31	7.00	190.09
CHON	13.12	101.04	1.56	194.27
ILOI	10.97	122.73	22.79	321.65
KUAL	5.32	103.14	2.49	63.75
NONN	16.00	108.26	3.21	226.53
PHUK	7.76	98.30	1.83	158.89
PUER	10.09	118.85	10.76	247.39
SURI	9.65	125.58	69.24	300.16
TANJ	-1.88	106.18	0.47	113.90
TEDA	0.57	97.82	31.76	359.19
VIRA	13.57	124.34	81.35	311.81
BRUN	4.97	115.03	10.92	287.68
AMPA	-1.01	121.44	53.90	307.54
DAVA	7.08	125.51	66.40	281.46
ENDE	-8.71	121.77	44.34	2.07
LAOA	18.52	120.60	100.35	283.99
TAWA	4.25	117.98	13.07	256.99
BALI	-8.15	114.68	4.61	308.98
LIRA	-8.06	125.74	58.60	6.40
MANA	1.33	125.06	19.35	309.78
AMBO	-3.78	128.12	50.98	335.77
BATU	-3.87	114.79	9.75	296.15
ZAMB	6.97	122.07	28.32	282.19
BUTU	-7.64	110.21	4.79	312.35
TOMI	0.45	120.85	92.67	318.86
UJPD	-5.15	119.58	6.86	355.67
TABA	0.86	108.89	2.77	59.60
KAPA	-9.78	124.28	59.07	5.31
WAME	-4.04	138.95	78.36	356.58
TOAR	-4.58	121.49	16.97	327.76
SANA	-2.05	125.99	65.87	307.04
TAIW	25.02	121.54	15.26	205.53
KEND	-4.23	122.74	22.84	325.93
REDO	-3.54	120.37	16.51	299.53

2 EASTWARD LIMIT OF THE UNDEFORMED SUNDALAND BLOCK

A major result of the GEODYSSSEA programme is the identification of an undeformed Sundaland block, because the stations NONN in Vietnam, PHUK and CHON in Thailand, PHUK and KUAL in Malaysia, MEDA and TANJ in Sumatra, and BAKO, BUTU and BALI in Java do not have significant relative motion (less than 3 mm yr⁻¹ on average, Figs 2 and 5, Chamot-Rooke *et al.* 1997, 1999). The absence of relative motion larger than 3 mm yr⁻¹ on average over a distance of up to 3000 km is an indication that the relative accuracy is comparable to the formal errors, as stated above. The undeformed Sundaland block includes the major part of the Indochina peninsula and Borneo as well as Java and

Sumatra. Presumably, it also includes the South China Sea, which is aseismic (see Fig. 1), although the GEODYSSSEA results cannot prove that the South China Sea is undeformed.

To the east, stations PUER, BRUN, TAWA and BATU reveal the existence of westward motion of about 10 mm yr⁻¹ with respect to Sundaland (Figs 2 and 5). The consistency in the direction of motion of these stations suggests that slow E–W convergence exists along the eastern boundary of the Sundaland block, from Palawan to southern Borneo. This convergence is confirmed by geological observations that reveal discontinuous thrust and fold zones in the Calamian Islands (North of Palawan), Brunei and the Meratus ranges (southern tip of Borneo). This discrete thrust belt could connect onshore Palawan along the N–S-trending Central Palawan Fault (Fig. 2), which extends southwards into the Sulu Sea. Station PUER is located on the hangingwall of this fault (Fig. 2). Seismological data in Brunei support the presence of active folding and reverse faulting that affect recent sediments on shore and onshore on the inner wall of the North Borneo Trench (NBT in Fig. 2: Hinz *et al.* 1989, Shell Co. 1996). Station BRUN is located on the overriding plate. This discontinuous thrust front extends in eastern Borneo within the upper Mahakam and the Meratus range, which is thrust westwards onto the Barito Basin (Pubellier *et al.* 1998a; see Fig. 2). Finally, this apparently aseismic thrust terminates southwards within the Java Sea (Fig. 13) along the western flank of the Lawrence Ridge. Station BATU is also located on the hangingwall of this NW-verging thrust zone. We consequently propose that about 10 mm yr⁻¹ of E–W shortening is accommodated immediately west of this discontinuous thrust front, extending from Palawan to the Java Sea, that marks the actual southeastern limit of undeformed Sundaland (see Fig. 2).

Note that, to the north, station CAMP in northern Vietnam has a 10 mm yr⁻¹ southward relative motion. CAMP is situated on the other side of the Red River Fault prolongation and actually belongs to the South China block (see Fig. 5; Chamot-Rooke *et al.* 1997; Le Pichon *et al.* 1997).

3 MOTION OF SUNDALAND WITH RESPECT TO AUSTRALIA AND PH

A second and even more important result of the GEODYSSSEA programme is the establishment of the fact that Sundaland at present does not belong to the Eurasia plate (EU). The motion with respect to Eurasia can be described by the SU/EU rotation given in Table 2 (Chamot-Rooke *et al.* 1997, 1999). It corresponds to an ENE velocity increasing from 10–15 mm yr⁻¹ to the south to 20–25 mm yr⁻¹ to the north, and consequently the motion with respect to the adjacent plates is significantly different from the motion with respect to EU, which was used in earlier kinematic and tectonic studies. Thus, the relative motion within the Australian collision zone is decreased (by approximately 5 mm yr⁻¹, from 76 to 71 mm yr⁻¹) and turned counterclockwise (by about 9° from 16°E to 7°E) when using the SU/AU motion instead of the EU/AU motion (Table 2, Fig. 4). Chamot-Rooke *et al.* (1997, 1999) have shown that the slip vectors of subduction earthquakes along the Java Trench are better adjusted with this new relative motion.

The motion with respect to PH is more uncertain because this plate is entirely surrounded by active subduction zones, thus the kinematics have been indirectly defined by partitioning

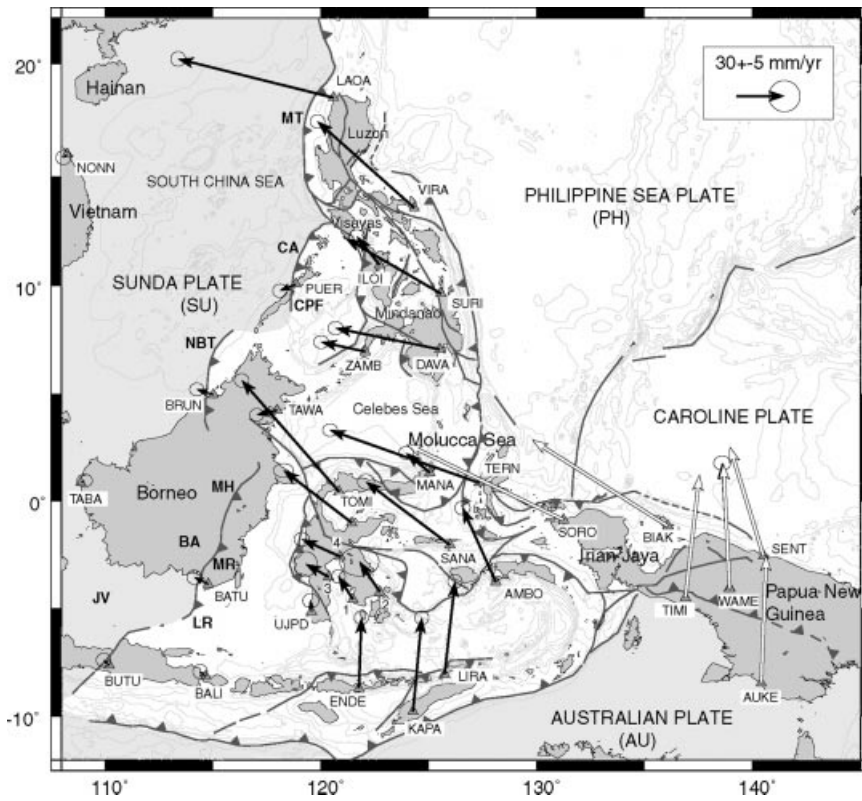


Figure 2. GEODYSSSEA GPS vectors with respect to Sundaland (black arrows). We have also included GPS vectors for Irian Jaya from Puntodewo *et al.* (1994; white arrows), recalibrated to fit GEODYSSSEA vectors (see text). 1 = TOAR, 2 = KEMB, 3 = REDO, 4 = MALI (see Fig. 12). NBT = North Borneo Trench, CA = Calamian thrust, CPF = Central Palawan Fault, MT = Manila Trench, MH = Mahakam thrust zone, MR = Meratus Range, BA = Barito Basin, LR = Laurence Ridge, JV = Java Sea.

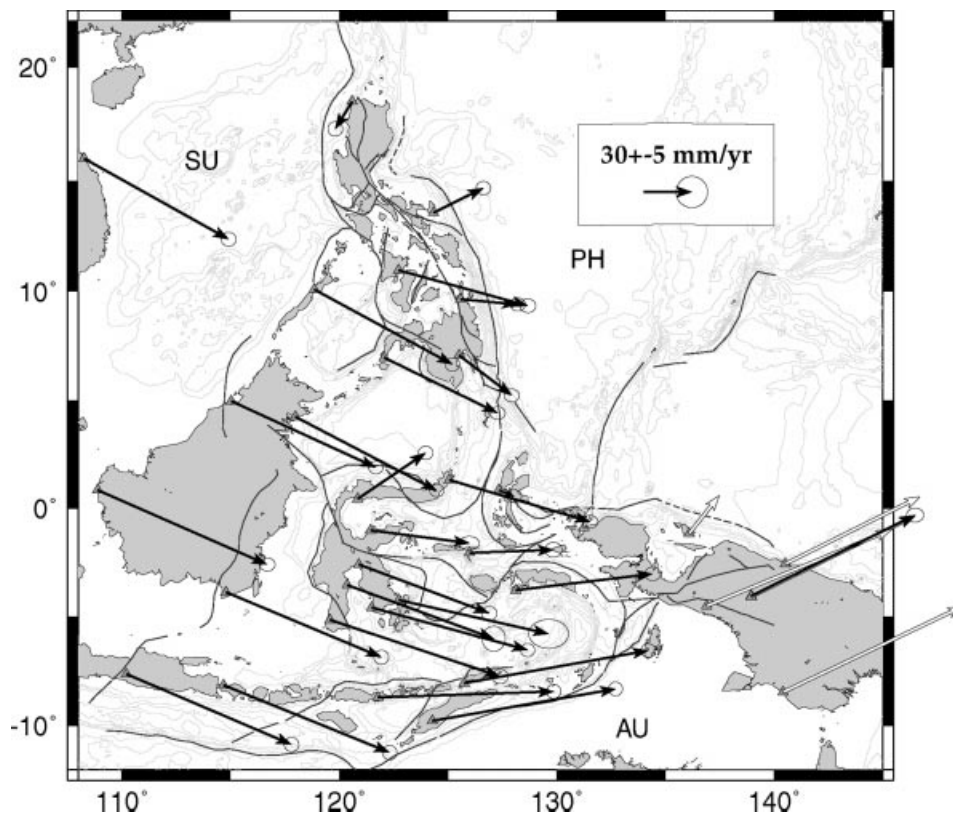


Figure 3. Same GPS vectors with respect to the Philippine Sea plate. SU = Sunda, PH = Philippine Sea Plate, AU = Australian Plate.

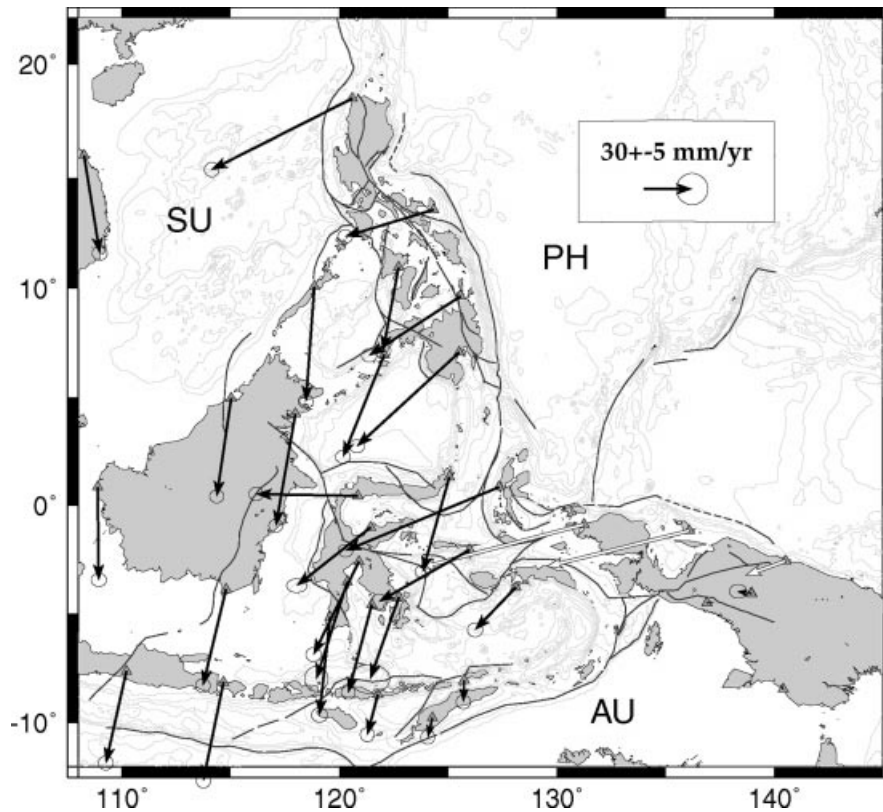


Figure 4. Same GPS vectors with respect to Australia. SU = Sunda, PH = Philippine Sea Plate, AU = Australian Plate.

Table 2. Rotation poles used in this study.

Rotation	Latitude°	Longitude°	Rate° Myr ⁻¹	Error Ellipse: σ_{\max} (°)/ σ_{\min} (°)/ ξ (°N)	Ref.
SU/E	33.23S	129.8E	-0.286		1
AU/EU	15.11N	40.45E	0.688		2
AU/SU	1.84N	60.17E	0.709		3
EU/PH	48.23N	156.97E	1.038		4
SU/PH	62.19N	169.81E	1.052		3
VI/SU	14.90	126.41	-3.600	2.33/0.71/75.28	5
LU/SU	9.34N	118.29E	5.478	0.23/0.16/-28.60	5
LU/PH	17.6N	122.1E	6.0		3
BA/SU	-6.93	118.85	2.671	0.63/0.33/51.89	5
BA/AU	8.3S	133.9E	2.35		3
SUL/SU	2.1N	126.2E	-3.4		6
LU/VI	11.5N	121.5E	9.07		3

1 Chamot-Rooke *et al.* (1999)

2 NUVEL1A

3 Derived from poles in this table

4 Seno *et al.* (1993)

5 This paper

6 Walpersdorf *et al.* (1998a)

the PA/EU motion on the two sides of the plates on the basis of slip vectors of subduction earthquakes. An additional constraint on the solution has been obtained by considering the rapidly changing tectonic relationship between PH and the Caroline Sea Plate along their common boundaries. The latest estimation of this type is by Seno *et al.* (1993). However, recent geodetic measurements have measured the displacement

vectors on two islands within the PH with respect to Eurasia (Chichijima and Parece Vela, Kato *et al.* 1996) and these measurements indicate that the PH kinematics proposed by Seno *et al.* (1993) are correct within the uncertainties of geodetic measurements. This is confirmed by the motion of a third island, Hachijojima, south of the Izu Peninsula, Japan, which has been obtained independently by the Geographic

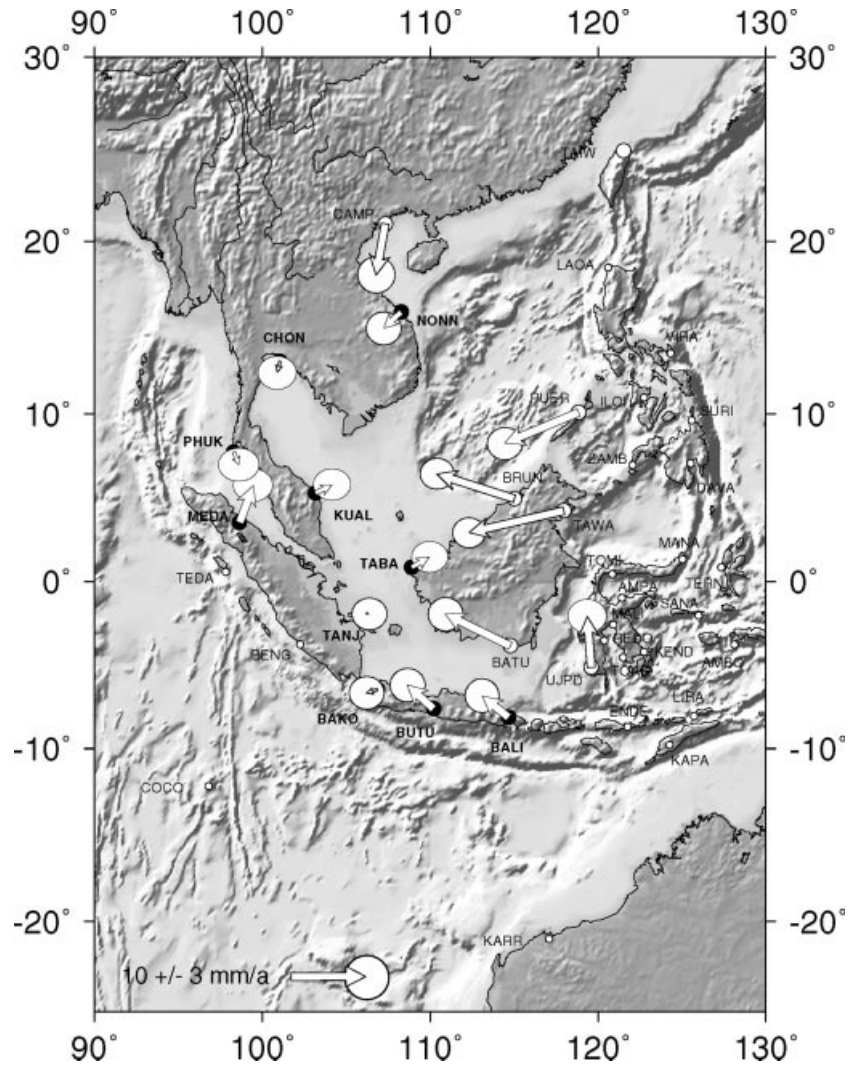


Figure 5. Residual vectors with respect to the Sunda block (from Chamot-Rooke *et al.* 1999).

Survey Institute of Japan (Miyazaki *et al.* 1997) as reported by Le Pichon *et al.* (1998) (see Table 3). Indeed, the rotation best fitting the three geodetic vectors shown in Table 3 is not significantly different from the Seno *et al.* (1993) rotation, the misfit in both cases being slightly more than 2 mm yr^{-1} , which is less than the probable errors. We will consequently adopt the rotation of Seno *et al.* (1993) recalibrated for the slight change in the timescale of the inversions as in NUVEL1A (DeMets *et al.* 1994). The resulting SU/PH rotation is given in Table 2 and the GEODYSSSEA vectors within the PH

Table 3. Philippine Sea Plate (PH) vector motion discussed in this study.

GPS site	Latitude (°)	Longitude (°)	Azimuth (°N)	V (mm yr^{-1})
HACHIJO	33,10	139,25	307,00	38.0
CHICHI	27,10	142,20	292,00	47.5
PARE C	20,40	136,03	300,00	60.0
TERN	0,86	127,34	294,37	82.8

framework are shown in Fig. 3. For example, the predicted convergence at station Ternate (Fig. 2, see location in Fig. 5), which can be considered as the westernmost part of the PH, just east of the Halmahera Trench, increases by 16 mm yr^{-1} and is slightly rotated counterclockwise by 4° with respect to the NUVEL1A PH/EU vector at the same location.

In fact, station Ternate (Fig. 3) provides an interesting test of the Seno *et al.* (1993) rotation. The motion there with respect to Eurasia is 10 mm yr^{-1} slower than predicted by their solution. This may be due to 10 mm yr^{-1} of shortening being absorbed east of Ternate in a diffuse convergence zone, although no well-defined active structure has been defined there, or to elastic loading on the Halmahera seismogenic zone. Alternatively, it is possible to fit the four PH geodetic vectors, including Ternate, with a comparable misfit of slightly more than 2 mm yr^{-1} , assuming that Ternate belongs to the PH and that elastic loading can be neglected (Table 2). This new rotation does not change the motion vectors in the northern part of the PH significantly but decreases them to the south. Thus, this test indicates that the kinematics of the PH are not yet fully established. The main constraint on the Seno *et al.* (1993) pole being the one they impose on the motion of PH

with respect to the Caroline Sea Plate to the south, it is probably safe to adopt their kinematics and to consider that the motion measured at Ternate is not the full PH motion. This appears to be confirmed by the fact that site LAOA in northern Luzon has a velocity compatible with the Seno PH velocity, as will be discussed later.

4 TECTONIC SET-UP OF THE PMB

This tectonic set-up will be described from north to south (Figs 6 and 7). The northeastern border of Sundaland, between southern Taiwan and Luzon, is an oblique convergence system: PH/SU convergence is mainly absorbed through eastward subduction of the South China Sea lithosphere along the Manila Trench. Convergence exists along the East Luzon Trough but it is minor as this trough is nearly entirely stifled by the arrival of the Benham plateau (Fig. 6; Karig 1973; Lewis

& Hayes 1983). South of Luzon, convergence flips to the other side of the Philippines and Luzon is consequently a broad zone of transfer from the eastward subduction of the Manila Trench to the northwest of the Philippines, to the westward subduction of the Philippine Trench to the southeast of this N–S-trending archipelago. We will attempt to show in this paper that this transfer occurs mostly through counterclockwise rotation of Luzon.

This rotation is limited to the south by a relatively simple system of faults. The left-lateral WNW/ESE Verde Passage Fault (Fig. 6, Marchadier & Rangin 1989) connects the Manila Trench to the west to the NE–SW Macolod Corridor to the east. The Macolod Corridor is a graben system along which the large volcanic calderas of Southern Luzon are built (Foster *et al.* 1990); it acts as a left-lateral pull-apart between the Verde Passage Fault to the SW and the left-lateral NW–SE Philippine Fault to the NE.

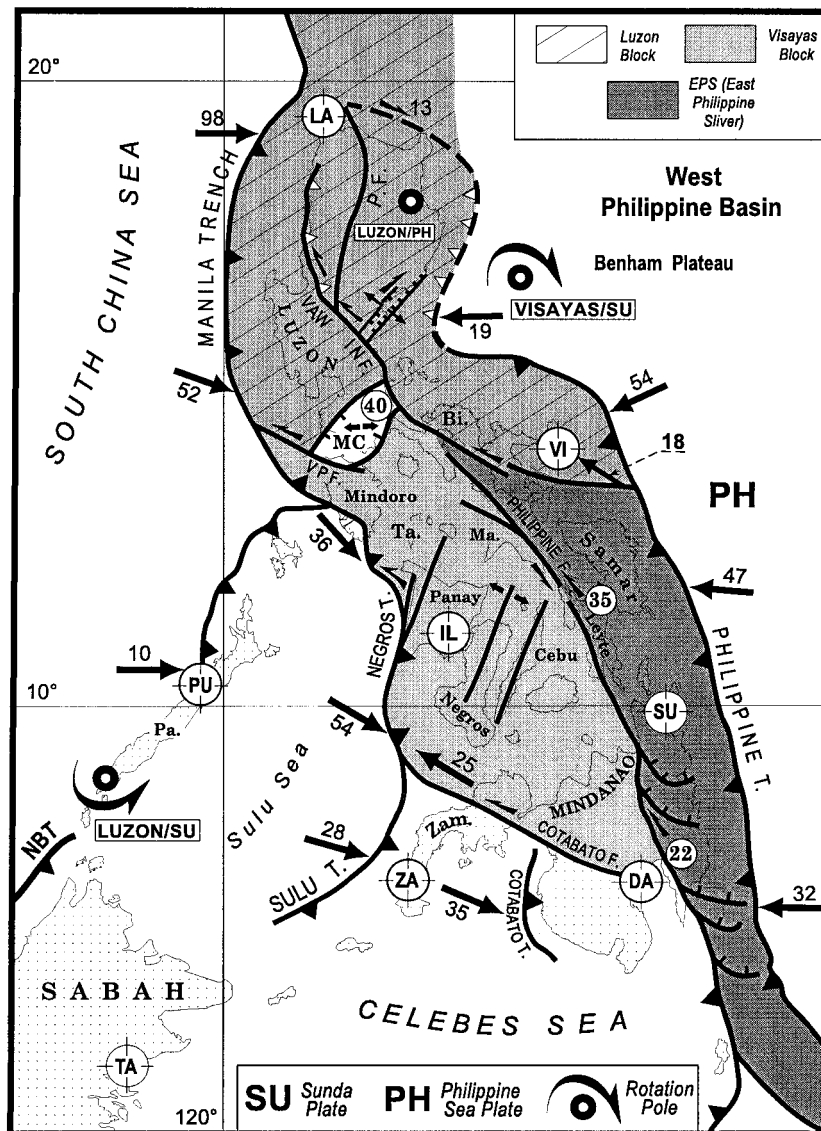


Figure 6. Distribution of the major tectonic boundaries and active mobile microblocks in the Philippines. GEODYSSSEA sites and their acronyms are shown. Estimated velocity vectors are given in mm yr^{-1} . GPS stations: LA = LAOA, VI = VIRA, PU = PUER, IL = ILOI, ZA = ZAMB, DA = DAVA, TA = TAWA; INF = Infanta Fault; Bi = Bicol peninsula; MC = Macolod Corridor; VPF = Verde Passage Fault; Ta = Tablas island; Pa = Palawan island; Zam = Zamboanga Peninsula; NBT = North Borneo Trench; PF = Philippine Fault; VAW = Vigan Agao Wrench Fault

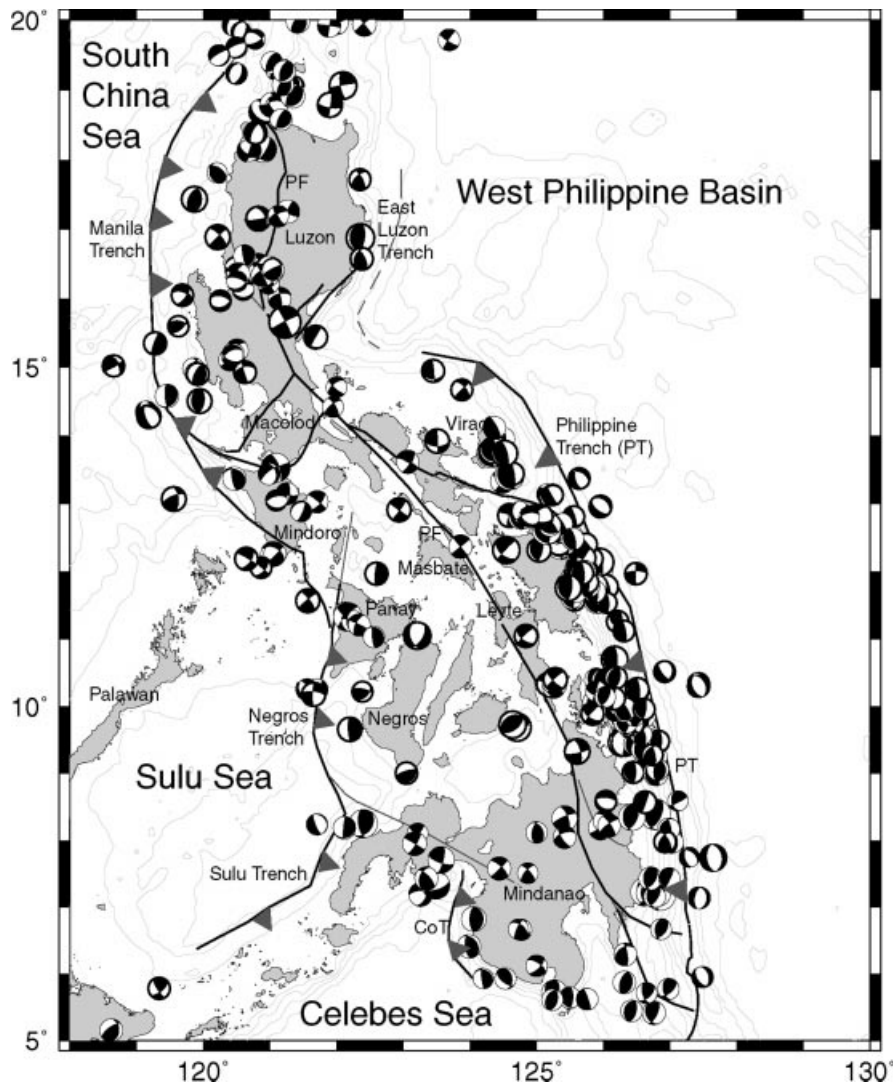


Figure 7. Fault plane solutions in the Philippines: CMT Harvard catalogue, 0–35 km, last 20 yr.

To the east, the Legaspi Lineament, an E–W fault merging with the Philippine Fault, extends to the Philippine Trench. It appears to take some limited left-lateral motion as well as some extensional motion (Le Rouzic & Gaulon 1997) (Fig. 6). To the north, the Philippine Fault has a northward left-lateral extension, known as the Infanta Fault, recently affected by a large seismic event (Ringgenbach *et al.* 1992). The left-lateral slip rate there should be smaller than the rate on the Philippine Fault by the amount of extension within the Macolod Corridor but was unknown when this paper was written. GPS data from Yu *et al.* (1999) now indicate that this rate is about 20 mm yr^{-1} .

The Infanta Fault follows the eastern coast of Luzon over about 100 km to branch northwards into two faults. Towards the NE, a dextral $N50^\circ E$ graben follows the southeastern coast (Ringgenbach *et al.* 1993) but its activity is unknown. This graben appears to control the location of the coastline in central Luzon (Fig. 6). Towards the NW, a left-lateral segment branches northwards into a system that dissects the Central Cordillera Cenozoic magmatic arc and the forearc sequence in Luzon into N–S elongated crustal slivers. The three different branches of this system are left-lateral with a dominating

westward thrusting component (Pinet & Stephan 1990). Pinet *et al.* (1990) proposed that only the western branch (the Vigan-Agao Wrench Fault, VAW in Fig. 6) is now active. However, the GPS data of Yu *et al.* (1999) indicate that the 20 mm yr^{-1} of left-lateral motion present along the Infanta Fault is absorbed along one or both of the eastern branches.

In the central and southern Philippines, the PMB extends from Luzon to Mindanao over a width of 500 km (Rangin *et al.* 1990a). It is fringed by opposing subduction zones (e.g. Hamburger *et al.* 1983). To the east, the West Philippine Basin is subducting towards the west along the Philippine Trench. Partitioning of the PH/SU motion is accommodated by left-lateral strike-slip faulting along the Philippine Fault. Part of the PH/SU convergence is absorbed to the west, on the opposite side of the PMB, along the Negro–Sulu–Cotabato trenches, where the Sulu and Celebes oceanic basins are subducting towards the east.

The PMB, jammed between these converging subduction zones and cut by the Philippine Fault, is under a compressive state of strain, marked by the distribution of thrusts and folds, particularly in the Visayas (Central Philippines, Rangin *et al.* 1989) and Mindanao (Southern Philippines, Quebral *et al.* 1996).

The present earthquake activity confirms that the state of stress is dominantly compressive or strike-slip with an E–W to NE–SW compressive axis (Fig. 7). However, as a first approximation, the largest faults divide the PMB into major crustal blocks that are relatively slowly deformed. The Verde Passage Fault, the Macolod Corridor and the central segment of the left-lateral Philippine Fault, discussed above, separate the Luzon block to the north from a Visayas block to the south. The Visayas block is fringed westwards by the Negros Trench and eastwards by the Philippine Fault. The southern boundary of the Visayas block is the Cotabato Fault, a left-lateral fault in Mindanao that extends from the Negros Trench westwards (Pubellier *et al.* 1996). In the central PMB, the East Philippine Sliver (EPS in Fig. 6) extends between the Philippine Trench to the east and the Philippine Fault to the west.

Further south, PH/SU convergence is mainly absorbed on both the eastern and western margins of the Molucca Sea (Figs 2 and 6), which subducts both westwards and eastwards along the Sangihe and Halmahera trenches, respectively. To the northwest of the Molucca Sea, no intraplate deformation is reported in the Celebes Sea (Hinz & Block 1990) or to the east, in the southernmost part of the West Philippine Basin (Hamilton 1978; Nichols *et al.* 1990). These two oceanic basin lithospheres can thus be considered to be undeformed. Nevertheless, in SE Sabah (Northern Borneo) active deformation is recorded on land in the Tawau area (Rangin *et al.* 1990b) and also offshore along the Sabah margin of the Celebes sea. This zone belongs to a more or less continuous slightly convergent belt at the eastern limit of the Sunda block, far from the Philippine–Molucca subduction zones, as discussed in the Introduction.

5 EVALUATION OF THE COSEISMIC AND INTERSEISMIC EFFECTS ON PHILIPPINE STATIONS AND SIMULTANEOUS EVALUATION OF THE SUBDUCTION MOTION ALONG THE PHILIPPINE TRENCH

Measuring the long-term secular motions of the major tectonic blocks in SE Asia was one of the main goals of the GEODYSSSEA project. To achieve this aim, the GPS sites have been selected in areas as far away as possible from active plate boundaries, so that the observed motions are unaffected by transient deformation related to earthquakes and consequently are representative of the secular motions of the corresponding tectonic blocks. However, due to the complex sea/land distribution and the difficult accessibility of many areas, not all of the sites could be installed at a sufficient distance from active block boundaries. We mainly discuss in the following sites DAVA, ILOI, SURI and VIRA, which are close to major plate boundaries; that is, the Philippine Fault and the Philippine Trench. We successively evaluate the coseismic and interseismic effects.

5.1 Coseismic effects

The major seismic events that have affected the measurements during the first phase of GEODYSSSEA (December 1994 until April 1996) were identified when computing the global solution of GEODYSSSEA (Wilson *et al.* 1998). The stations clearly affected by coseismic effects are BIAK (Irian Jaya) and TOMI (Sulawesi). They have been discussed by Walpersdorf *et al.*

(1998a) and Michel *et al.* (1998a,b). The corresponding effects are so large that the secular motion is very difficult to obtain at these stations; consequently, we will not use them in our analysis. LAOA, in northern Luzon, was affected by a magnitude 5.4 intermediate-depth earthquake that occurred at an epicentral distance of about 30 km. The results were thus suspected to be affected by strong coseismic motion (Wilson *et al.* 1998). Since then, Michel *et al.* (1998a,b) have shown that any coseismic effect cannot exceed a few millimetres. In addition, they pointed out that the LAOA velocity obtained, which is a PH velocity (see Fig. 4), is comparable to velocities measured in the vicinity of this station within Luzon by Yu *et al.* (1999). This site will consequently be used in our analysis.

However, several sites located in the central Philippines (DAVA, ILOI, SURI and VIRA, see Fig. 2) might have recorded the effects of some much more limited coseismic transients, due to five large subduction earthquakes ranging from M_s 6.8–7.1, which we consequently need to evaluate (Michel *et al.* 1998a,b). We compute the surface velocity field associated with these earthquakes with the help of a dislocation model in an elastic half-space (Okada 1992). The earthquake parameters are derived from the Harvard CMT data bank. We use the Wells & Coppersmith (1994) empirical correlation laws between the moment magnitude (M) and the slip to define an average displacement along the fault. We set the downdip length of the fault surface to the maximum extent of the observed seismogenic zone (about 74 km offshore Samar island between VIRA and SURI). The lateral width of the plane is defined through the equation that links the seismic moment M_0 (dyne cm⁻¹) to the fault surface S (km²), the shear modulus μ ($\mu = 3.1011$ dyne cm⁻² for crustal faults) and the slip along the fault D (cm): $M_0 = \mu S \times 10^5 D$.

Table 4 shows the parameters used for the three most significant earthquakes. The predicted motions at the three sites VIRA, SURI and ILOI are shown in the last three columns. The coseismic motion produced by the largest earthquake (1995 April 21, M_s 7.1) is shown in Fig. 8. At the three stations, it is of the order of a few millimetres. If we add up the contributions of the five earthquakes, the total coseismic motion predicted at these three stations remains small, the largest possible effect being about 5 mm at ILOI, in spite of the fact that it is slightly more distant than VIRA and SURI, because ILOI is in the direction of motion of the faults (see Fig. 8). In view of the uncertainty on the Harvard parameters, the magnitude and direction of the predicted motions are not well determined and only an approximate correction of the GPS data is possible. Fortunately, the coseismic effects of this series of earthquakes on the GPS data are a few millimetres and thus fall within the error bars of the data, except at ILOI.

Following the earthquake instantaneous coseismic motion, post-seismic motion may occur. Recently, Heki *et al.* (1997) showed that the cumulative, presumably elastic, post-seismic motion following the offshore-Sanriku earthquake along the Japan Trench in 1994 ($M_w = 7.6$) was of the same order of magnitude as the coseismic motion after 1 yr. Thus, we cannot exclude the possibility that the GEODYSSSEA GPS measurements there may have been affected by post-seismic transients following one or several of the major earthquakes discussed, although there is no indication yet about the frequency of this type of slow post-seismic energy release. In the worst case, the post-seismic transients may have been of the same order of magnitude as the coseismic motion after 1 yr. We conclude that the

Table 4. Earthquake parameters and predicted site motions. Latitude and Longitude: coordinates of the earthquake; Az, Dip, Wid. and Len.: azimuth, dip, along-strike width and downdip length of the fault; Slip/Az: magnitude and azimuth of the slip on the fault; V_x , V_y and V : east and north components and norm of the predicted motion.

Earthquake event	Lat (deg)	Lon (deg)	Az (deg)	Dip (deg)	Wid. (km)	Len. (km)	Slip (mm)/Az	Site (deg)	V_x (mm)	V_y (mm)	V (mm)
21/04/95 <i>M_s</i> 7.1	12.06	125.93	N153	22	46	74	440 N272	VIRA	1.29	-0.47	1.37
								SURI	0.25	0.21	0.33
								ILOI	1.72	0.51	1.79
21/04/95 <i>M_s</i> 6.8	12.00	125.70	N150	17	26	74	280 N268	VIRA	0.24	0.07	0.24
								SURI	0.07	0.08	0.10
								ILOI	0.64	0.20	0.67
05/05/95 <i>M_s</i> 7.0	12.62	125.31	N145	16	38	74	380 N260	VIRA	1.07	-0.34	1.12
								SURI	0.08	-0.03	0.08
								ILOI	1.13	0.65	1.30
Cumulative effect of the 5 major earthquakes								VIRA	2.60	-0.74	2.73
								SURI	0.40	-0.26	0.51
								ILOI	3.49	1.36	3.76

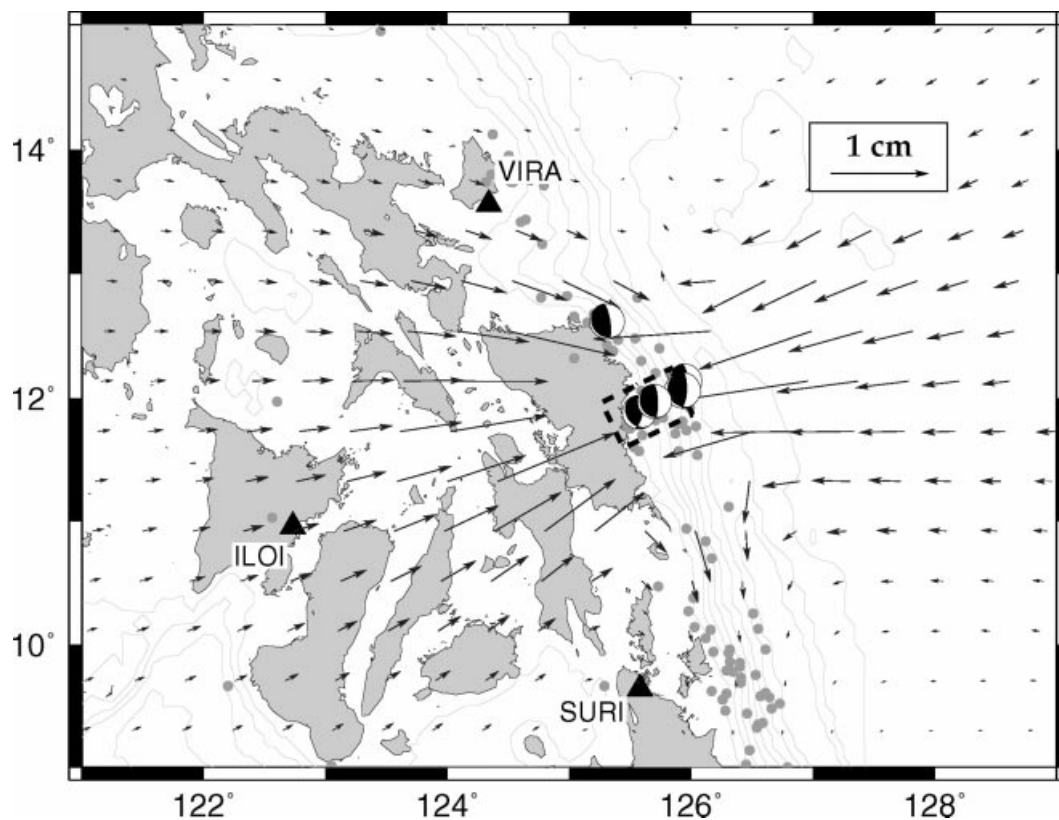


Figure 8. Coseismic surface displacement field related to the 1995 April 21, M_s 7.1 earthquake. The rupture surface associated with this earthquake (fault dimensions: 74×46 km; slip: 68 cm towards N272°) is shown by a dashed rectangle. The predicted displacement field due to the seismic rupture is shown by black arrows. The five earthquakes discussed in the text are represented by their focal mechanisms, and intraplate subduction earthquakes from 1977 to 1998 are represented by grey dots.

maximum amplitudes of the possible transients recorded by the stations would be about twice the values in Table 4, although we consider it extremely unlikely that these maxima would have actually occurred.

To summarize, we consider that the cumulative coseismic and post-seismic effects of the 1995 earthquakes can be ignored at sites VIRA and SURI, where the probable predicted motions should be a few millimetres. This estimate should be increased to 10 mm at ILOI and we will consequently make this correction

for ILOI, knowing that it is poorly determined. The adopted velocity at ILOI, after correction for the cumulative coseismic effect, is 25 mm yr^{-1} towards 305° .

5.2 Interseismic effects

GPS sites DAVA, ILOI, SURI and VIRA are located at, respectively, 90, 140, 200 and 400 km from the Philippine Trench axis. If the subduction plane is locked, part of the

motion detected at these GPS sites may correspond to elastic loading of the PMB by the Philippine Sea slab. To test this possibility, we compute the interseismic elastic velocity field produced by a locked slab. Following Savage (1983), we describe the interseismic phase by a combination of steady-state slip along the fault surface (reverse motion) and a dislocation in the opposite direction (normal motion) along the locked portion of the fault. In this model, the displacements are computed with respect to a fixed Sunda plate, and the Philippine arc shows motion towards the west during the interseismic phase. We use a geometry of the locked subduction zone derived from the seismicity observed along the Philippine Trench (average dip: 20° towards the west; downdip length: between 80 and 70 km; depth of the lower edge: 24 km).

We now need to estimate the convergence motion between the Philippine Sea plate (PH) and the Philippine Mobile Belt (PMB). To do this, we subtract the GPS measured motions at sites VIRI and SURI (in the SU reference frame, see Table 5) from the PH/SU predicted motions. The resulting vectors are interpreted as the PH/PMB motion. If we consider that the

GPS data include the elastic motion that corresponds to a locked subduction, the predicted PH/PMB motion must be corrected for the corresponding elastic loading. We estimate this correction by computing the elastic displacement predicted at the two sites and correct the PH/PMB convergence with the estimated elastic effect. We then iterate this 'elastic loading/correction' process, which leads to a PH/PMB motion and an elastic correction motion that converge to the values shown in Table 5. The actual long-term motion is either the vector corrected for the transient effect, if the subduction zone is locked, or the vector without any transient correction, if it is slipping.

The results are shown in Fig. 9. The VIRI GPS vector corrected for the elastic loading is rotated clockwise by 13° but the modulus is decreased by 4 mm yr^{-1} . The motion absorbed along the Philippine Trench is normal to the trench at VIRI (241°) and nearly parallel to the slip vectors there ($256^\circ \pm 8^\circ$, according to McCauley 1996), which confirms the existence of full partitioning of the PH relative motion (Barrier *et al.* 1991). The variation in azimuth is 5° for SURI and the

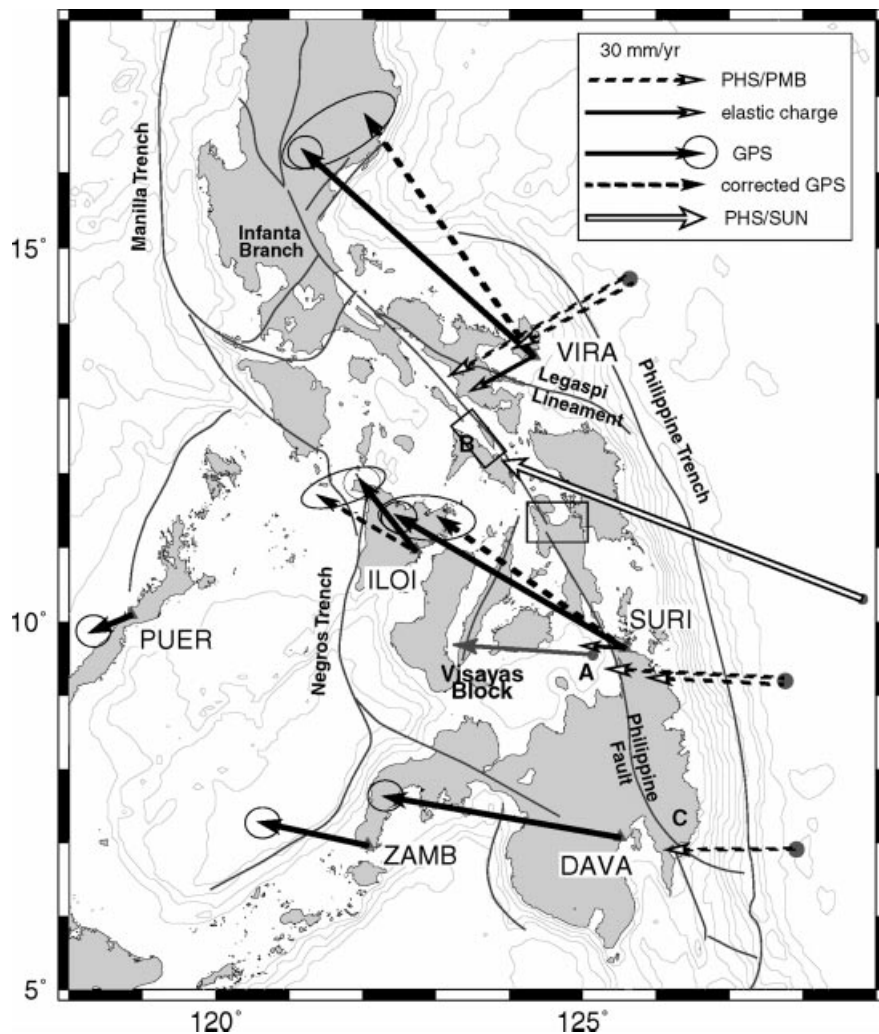


Figure 9. GPS motion and potential elastic loading of the Philippine Sea slab in the Central Philippine area. White arrow: Philippine Sea with respect to Sunda plate motion. Thick black arrows: GPS vectors with respect to the Sunda plate. White-headed arrows: convergence velocity along the Philippine Trench (with respect to the Philippine Mobile Belt) and predicted full coupling interseismic charge at GPS sites VIRI, SURI and DAVA. Thick dashed arrows: GPS vectors corrected for the potential elastic loading maximum effect. The range of corrected GPS data falls within the large ellipse. Thin black lines: major active faults.

Table 5. Convergence motion, elastic loading motion and GPS corrected motion estimated at the GPS sites in the Central Philippines. Lat, Lon: coordinates of the stations; PH/PMB convergence: slip along the Philippine Trench; Elastic loading: transient elastic charge at the GPS sites predicted for a fully locked Philippine Trench; Corrected GPS: GPS vectors corrected from the elastic motion.

Site	Lat. (deg)	Lon. (deg)	Measured GPS (mm yr ⁻¹ , deg)	PH/PMB convergence (mm yr ⁻¹ , deg)	Elastic loading (mm yr ⁻¹ , deg)	Corrected GPS (mm yr ⁻¹ , deg)
VIRA	13.57	124.34	81 N312	35–54 N241	19 N241	77 N325
SURI	9.65	125.58	69 N300	36–47 N273	11 N273	59 N305
DAVA	7.08	125.51	66 N281	40–44 N304	4 N304	62 N280

modulus is reduced by 10 mm yr⁻¹. The 273° motion absorbed in the Philippine Trench is also parallel to the slip vectors there (269° ± 12°, McCa rey 1996) and also nearly normal to the trench. The velocity of subduction decreases from 54 mm yr⁻¹ (35 mm yr⁻¹ with the trench unlocked) near 14°N to 47 mm yr⁻¹ (36 mm yr⁻¹ with the trench unlocked) near 10°N. The subduction velocity, with the trench unlocked, is only a minor portion of the PH/SU velocity and would imply that the larger portion of this motion is absorbed to the west of the Philippines, whereas the seismicity (see Fig. 7) suggests the reverse. This appears to indicate that the Philippine Trench subduction zone is locked. We will present other indications that locking of the seismogenic zone seems to fit several tectonic observations better. We will consequently use the vectors corrected for interseismic loading effects.

We now test the types of solutions obtained for subduction in the Philippine Trench if it is assumed that the undeformed part of SU is actually part of Eurasia, as was generally assumed prior to the GEODYSSSEA programme. We should then use the PH/EU rotation to derive the convergence motion across the Philippine Trench of the latitudes of VIRA and SURI. However, the results obtained do not fit the directions of the slip vectors. For example, for VIRA the azimuth of the derived subduction vector is 208° instead of the 256° ± 8° expected. For SURI the azimuth obtained is 245° instead of the 269° ± 12° expected. The differences in azimuths are significant because the azimuths of the subduction vectors obtained do not vary significantly between the two solutions (trench locked and trench unlocked), as the subduction vector and the elastic loading vector onshore of the trench are essentially parallel. In addition, the velocity of subduction of about 15 mm yr⁻¹ obtained appears unrealistic in view of the large amount of seismicity there. Because the relative motions of the PMB with respect to SU appear to be quite robust, this indicates that SU does not belong to EU but that it has a significant velocity of the order of 15–25 mm yr⁻¹ to the east with respect to EU, as found by the GEODYSSSEA programme. Chamot-Rooke *et al.* (1997, 1999) have previously shown, using the slip vectors in the Java Trench and in Sumatra and the geology in Burma, that this conclusion also applies to the southern and western borders of Sundaland. This is now confirmed by the Yu *et al.* (1999) data, as there are no systematic differences between the Yu *et al.* (1999) GPS vectors and the GEODYSSSEA data at the four sites (Taiwan, PUER, VIRA and LAOA) that are common to both networks.

The DAVA site is located on the western side of the Philippine Fault but the N–S orientation of the Philippine Fault in this area predicts that the motion along it which is

produced by partitioning of the PH/PMB motion, is small. This is verified by the fact that this fault progressively dies out to the southeast of DAVA (Pubellier *et al.* 1999). Knowing the slip vector direction in the trench near 7°N, 270° ± 10° (Fig. 6), we can solve for the Philippine Fault slip rate that produces the proper subduction direction (Fig. 10a). This is done by finding the slip rate that produces a velocity at point C (location in Fig. 9), opposite DAVA, on the east side of the Philippine Fault such that the relative motion in the subduction zone should be E–W. The slip rate on the fault is then 22 mm yr⁻¹, and the rate of subduction in the trench is 32 mm yr⁻¹. The elastic correction is only 3 mm yr⁻¹.

Thus, the rate of subduction continuously decreases from north to south along the Philippine Trench from 54 mm yr⁻¹ near 13°N, to 47 mm yr⁻¹ near 10°N and finally to 32 mm yr⁻¹ near 7°N, assuming that the subduction zone is locked. On the other hand, the subduction rate is constant at about 35 mm yr⁻¹ if the trench is unlocked. The progressive decrease southwards when the trench is locked is another reason to assume that it is indeed locked as it is known that the Philippine Trench dies out southwards near 4°N (Lallemand *et al.* 1998).

6 EVALUATION OF THE MOTION ABSORBED ALONG THE MAIN TECTONIC BOUNDARIES WITHIN THE PMB

6.1 The Philippine Fault

The Philippine Fault is a major left-lateral strike-slip fault active all along the Philippine archipelago from Luzon to Mindanao. GPS studies have been carried out near 11°N on Leyte Island and near 12.5° on Masbate island and two smaller islands further north (see Fig. 9; Duquesnoy 1997). Early results indicated a slip velocity of 26 ± 6 mm yr⁻¹ on Leyte (Duquesnoy *et al.* 1994). A longer set of measurements now gives 35 ± 4 mm yr⁻¹ (Duquesnoy 1997). The velocity within the central segment of the Philippine Fault on Leyte and Masbate thus appears to be close to 35 mm yr⁻¹ (Duquesnoy 1997). This is the velocity we use within the triangle formed by stations VIRA, ILOI and SURI. Near the latitude of SURI, the fault progressively takes a N–S orientation and presumably simultaneously reduces its slip velocity, although we have no direct indication of this reduction. At the latitude of DAVA, we derived previously a lower velocity of 22 mm yr⁻¹ and the fault indeed dies out to the south of DAVA, because an onshore multibeam survey was unable to locate the fault trace south of Mindanao (Bader *et al.* 1999). The increase in velocity from

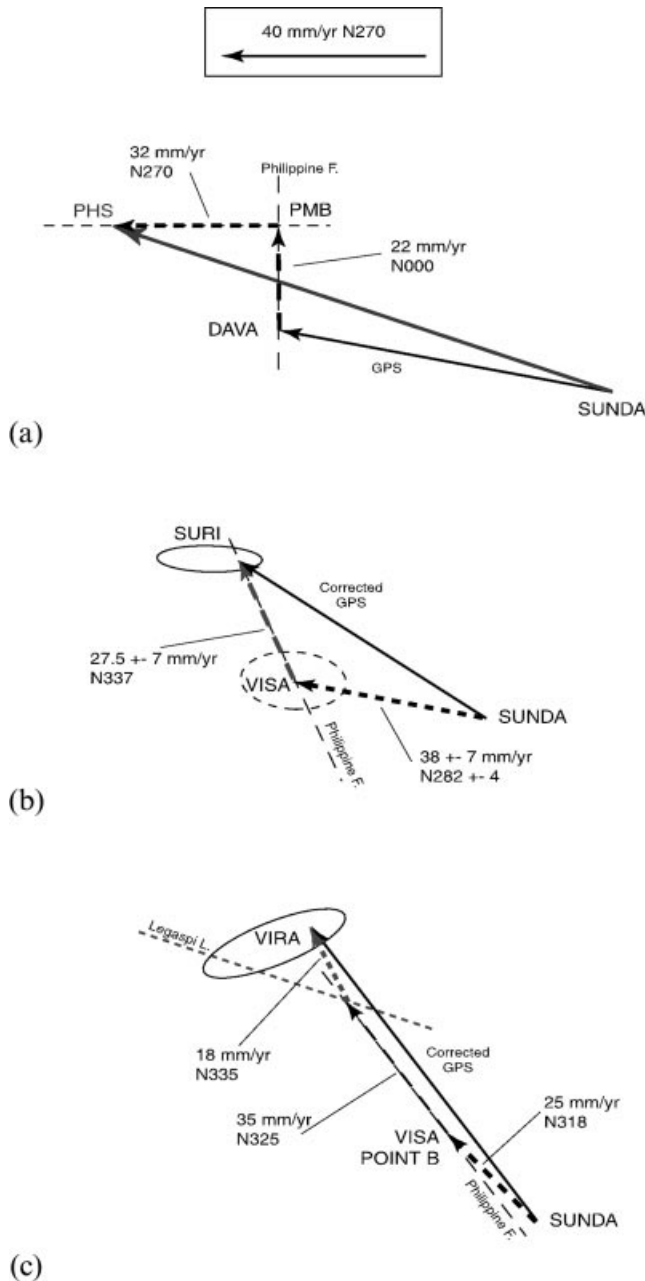


Figure 10. Vector diagrams on three sites of the PMB. (a) South Mindanao (GPS site DAVA); (b) north Mindanao (GPS site SURI); (c) south Luzon (GPS site VIRIA).

0 to 35 mm yr⁻¹, between south of 7°N and 10°N, is obtained through zones of extension connecting the fault to the Philippine Trench (Pubellier *et al.* 1996; Quebral *et al.* 1996).

The detailed GPS surveys mentioned above indicate that this central segment of the fault was not locked while the GEODYSSSEA measurements were made (Duchesnoy 1997). Thus, we should not expect any interseismic elastic deformation near the fault there. We next show that any possible such effect would be small anyway at the GEODYSSSEA stations considered, even if the fault is locked. Our model assumes a pure strike-slip fault between two blocks (Savage 1983). The model parameters are the locking depth and the far-field velocity across the fault. The downdip extent of the seismogenic zone in

the south Luzon segment of the fault is estimated to be 15 km (Shibutani *et al.* 1991). With the help of this model, we have evaluated the effect of a locked Philippine Fault on stations DAVA, SURI and VIRIA, at distances of 40, 15 and 120 km, respectively, from the fault. At these distances, the expected effects of the locking of the fault are, respectively, 3, 7 and 1 mm yr⁻¹. We can consequently safely assume that any transient effects related to the Philippine Fault, during this period and at the GEODYSSSEA sites considered, can be neglected.

6.2 The Visayas block

Knowing the 35 mm yr⁻¹ slip rate along the 11–13°N segment of the Philippine Fault and the 22 mm yr⁻¹ slip rate at 7°N, the left-lateral motion along the fault at the latitude of SURI should lie between these two values. We consequently assume a value of 27.5 ± 7 mm yr⁻¹ towards 337° to derive the motion of point A on the Visayas block, immediately west of SURI, on the other side of the fault (Fig. 9). The vector obtained is 38 ± 7 mm yr⁻¹ towards 282 ± 4° (see Fig. 10b). We then know the motions of three points on the Visayas block, point A, DAVA and ILOI, and we can evaluate the kinematics of this block.

Fig. 9 indicates that the three vectors appear to show a clockwise rotation with a pole to the NNW. In this rotation, point A and ILOI should be approximately at the same Eulerian latitude. However, the velocity of ILOI is 18 mm yr⁻¹ less than the velocity of point A. This suggests that the Visayas block is affected by shortening oriented E–W to SE–NW. Seismological observations confirm this suggestion (Fig. 7) as well as geological observations (Rangin *et al.* 1989). We neglect however, this deformation in a first approximation to obtain the approximate motion of the Visayas block with respect to SU, using the three vectors at point A, DAVA and SURI. The rotation fits the three azimuths quite well; the misfit with the DAVA vector is 8 mm yr⁻¹ and that with the ILOI vector is 13 mm yr⁻¹. The fit with ILOI deteriorates significantly without the coseismic correction. We thus adopt for the Visayas block motion with respect to SU the rotation given in Table 2. The rotation pole is located 2° east of the northern extremity of the Philippine Trench (Fig. 6). The rotation is clockwise and the rate is 3.6° Myr⁻¹. The ellipse gives an estimate of the uncertainties (see Table 2). McCabe *et al.* (1982) have reported from palaeomagnetic measurements the existence there of a 20° clockwise rotation. It could have been produced in 5.5 Myr at the present rate of rotation. However, they report that the Upper Miocene to Pleistocene formations show no evidence of rotation and they conclude that the palaeomagnetically measured rotation is post-Oligocene and pre-Upper Miocene. If this is confirmed, it suggests that the present rotation does not exceed 10° and consequently has not been active for more than 3 Myr.

Comparing the predicted motion in ILOI to the actual measured motion, we find that 13 mm yr⁻¹ towards 325° should be absorbed within the Visayas block. This shortening is at the limit of resolution of the measurements, in view of the different corrections made to derive it, and cannot be considered established solely from these geodetic measurements. However, it does fit independent seismological and tectonic data, as discussed above.

6.3 The Negros Trench

If the Sulu Sea belongs to SU, the motion just defined for the Visayas block predicts an average 45 mm yr^{-1} towards 315° for the convergence rate along the Negros Trench, the rate increasing from north to south from 36 mm yr^{-1} towards 325° near 12°N to 54 mm yr^{-1} towards 303° near 8.5°N (see Fig. 6). Station PUER, however, indicates a motion of about 10 mm yr^{-1} towards 250° for Palawan with respect to SU, which is probably significant, as discussed earlier. Because the Palawan block may be affected by significant unknown rotation with respect to the Philippines, we cannot correct exactly for the motion of PUER, and the estimates of convergence attributed to the Negros Trench are overestimated by somewhat less than 10 mm yr^{-1} .

The part of the Negros Trench between 10.5°N and 12°N is now starved by the collision with the Palawan continental block on northern Panay Island, where the oblique convergence along the Negros Trench is partly transferred to the oblique NW-trending Manila Trench south of Mindoro (Marchadier & Rangin 1989). The presence of active left-lateral faulting there is also supported by the fault plane mechanisms (Fig. 7). The Manila Trench is waning rapidly southwards of the Verde Passage Fault opposite Mindoro towards the Palawan collision zone.

To the south, site ZAMB indicates that 28 mm yr^{-1} towards 280° is absorbed by subduction in the Sulu Trench towards the west. Thus, the Cotabato Fault, which forms a triple junction with the Sulu Trench and the Negros Trench, should be left-lateral with a slip rate of about 25 mm yr^{-1} . About 35 mm yr^{-1} of convergence should be absorbed between the Cotabato Trench, which is in the prolongation of the Cotabato Fault, and the Central Range of Mindanao, based on the DAVA and ZAMB vectors.

6.4 The Luzon block and the Manila Trench

We will first show that the motion at site LAOA in northernmost Luzon is close to the motion of PH. As the GEODYSSSEA data do not enable us to differentiate between Eastern and Western Luzon along the northernmost branch of the Philippine Fault (Pinet & Stephan 1990), we consider that Luzon forms a relatively undeformed block and determine its kinematics with respect to SU. We will then consider the kinematics with respect to PH and finally with respect to the East Philippine Sliver and the Visayas block. As we were revising this paper, the Yu *et al.* (1999) data were published. They have confirmed that the northern Luzon block, east of the Philippine Fault, is essentially undeformed. However, these data also demonstrate that there is about 20 mm yr^{-1} of left-lateral motion along the northern branch of the Philippine Fault. Thus, the northwestern Luzon block, west of the northern branch of the Philippine Fault, has a motion that differs from that of the northeastern Luzon block. The existence of this block in our kinematic model is ignored but we have verified that its introduction would not change the main conclusions obtained with our simpler model.

On the east side of northern Luzon, the Philippine Trench appears to be starved by the arrival of the Benham Plateau within the trench (Karig 1973). Most of the convergence motion should then be absorbed along the Manila Trench to the west by eastward subduction of the South China Sea

lithosphere. Thus we would expect northern Luzon to be moving at the velocity of the PH. This is verified by the motion at LAOA, at the northeastern extremity of Luzon, which is 100 mm yr^{-1} towards 284° , equivalent to the velocity of PH there (99 mm yr^{-1} towards 294° , see Fig. 2), with a clockwise rotation of 10° . We do not attempt to correct for possible elastic loading in the Manila Trench as the correction of this effect would actually increase the westward motion, which is already slightly larger than the PH motion. This suggests that the seismogenic zone there is unlocked and the data of Yu *et al.* (1999) now appear to confirm this point. We simply take the LAOA vector as an indication that the northernmost portion of Luzon belongs kinematically to the Philippine Plate and that the whole PH motion is absorbed within the northern Manila Trench, the East Luzon Trough being thus completely inactive to the north. To the south, the East Luzon Trough could absorb some limited convergence, as shown by fault plane solutions of earthquakes (Fig. 7) and seismic surveys (Lewis & Hayes 1983), and the rate of subduction within the Manila Trench must decrease accordingly southwards.

We next consider site VIRA in SE Luzon and compare it to LAOA. It turns out that VIRA is stationary with respect to LAOA. In other words, the LAOA and VIRA vectors with respect to EU can be exactly fitted (to better than 1 mm yr^{-1}) by a single counterclockwise rotation, the Eulerian pole being situated in southern Palawan (LU/SU: 9.3°N , 118.3°E , $5.5^\circ \text{ Myr}^{-1}$, Table 2). Although the perfect fit must be attributed to a coincidence in view of the probable errors, the fact that there is a good fit is an indication that both sites belong to the same relatively undeformed block, which includes northern and southeastern Luzon. This block rotates counterclockwise at the relatively fast rate of $5.5^\circ \text{ Myr}^{-1}$, thus explaining entirely the difference in modulus of 23 mm yr^{-1} as well as the difference in direction of 41° . The LU/SU rotation predicts that subduction in the Manila Trench is towards 100° at a rate decreasing from 100 mm yr^{-1} opposite LAOA to 50 mm yr^{-1} at its southern extremity, near 14°N .

A 20° – 30° counterclockwise rotation was detected by palaeomagnetic studies there (McCabe *et al.* 1982), which could be the result of 4–6 Myr of the present rotation, which would be geologically reasonable. However, the age of the palaeomagnetic rotation is reported as post-Oligocene and pre-Upper Miocene, the same as within the Visayas. Thus, if this dating is correct, the present finite rotation should be less than 10° and should accordingly have started at less than 2 Ma.

6.5 The motion of the Luzon block with respect to the PH

The LU/PH rotation derived has its pole on the northeastern coast of Luzon and the 6° rotation rate is counterclockwise (Table 2 and Fig. 6). The predicted convergence vector is zero to the north of East Luzon Trough and increases to 19 mm yr^{-1} to the west at its southern extremity. The predicted motion is then 30 mm yr^{-1} of left-lateral movement along the 15°N E–W continental margin, and the predicted subduction opposite site VIRA is of course the same as obtained directly earlier, as VIRA motion is taken into account exactly in the adopted kinematics of the Luzon block. It is clear that the East Philippine Sliver does not obey the same kinematics because the predictions of subduction along the trench start diverging from the previous estimates south of the Legaspi Lineament.

We will return to this lineament below. Finally, on the northern coast of Luzon the predicted motion is 13 mm yr^{-1} in a right-lateral sense along 260° , which appears to fit the fault plane solutions obtained there (Fig. 7), in spite of the small value of the vector obtained.

6.6 The Legaspi Lineament and the East Philippine Sliver

Broadly speaking, the northeast counterclockwise motion of the Luzon block is directly continuous with the NNE motion of the East Philippine Sliver. To test this point more precisely, we will next try to evaluate the motion along the Legaspi Lineament. From the analysis of the Visayas block motion, we obtain the velocity in the northern portion of the Visayas block, at point B, immediately south of the Masbate GPS survey, where a slip rate of 35 mm yr^{-1} was determined along this segment of the Philippine Fault. This velocity at point B is about 25 mm yr^{-1} towards 318° (Figs 9 and 10c). Along a transect from point B to site VIRA, the differential motion between the two points should be absorbed along the Philippine Fault, where the slip rate is known, and along the Legaspi Lineament. We can then deduce the motion occurring along the Legaspi Lineament (see Fig. 10c). The Legaspi Lineament is seismically active and is a left-lateral fault with a normal component of motion to the east (Le Rouzic & Gaulon 1997; see Fig. 7).

The corresponding motion that we obtain on Legaspi is 18 mm yr^{-1} towards 335° . Because the orientation of the Legaspi Lineament is about 290° along this section, this solution implies 13 mm yr^{-1} of left-lateral motion along the Legaspi Fault with 13 mm yr^{-1} of extension perpendicular to it. Note that the indirect estimate of the velocity at point B, in the northern portion of the Visayas block, is quite uncertain and that consequently the velocity derived on the Legaspi may be within the uncertainty range.

Nevertheless, the motion on the Legaspi determined above predicts a velocity of 60 mm yr^{-1} towards 322° on the southern side of the Legaspi Lineament. This velocity is compatible with the 59 mm yr^{-1} velocity of site SURI on the Eastern Philippine Sliver to the south, with a clockwise rotation of 17° due to the rotation of the Visayas block. As a result, the direction of 322° is parallel to the Philippine Fault at this latitude, confirming that, although the Legaspi Lineament helps to increase the velocity of transfer of the Eastern Luzon block to the NW, the northeast counterclockwise motion of the Eastern Luzon block is actually in direct continuity with the NNE motion of the Eastern Philippine Sliver. This system transfers the northward motion obtained by strain partitioning along the Philippine Trench to the Manila Trench in a broad counterclockwise rotation over a length of 1300 km (see Fig. 6).

6.7 Luzon motion with respect to the Visayas block

The system of transfer of motion between the Luzon block and the Visayas block includes the Verde Passage Fault, the Macolod Corridor and the portion of the Philippine Fault near 14°N . The total motion to be absorbed as given by the rigid approximation is the LU/Visayas rotation (Table 2 and Fig. 6). The pole of rotation is situated south of Mindoro and west of Panay. The rate of rotation is 9° Myr^{-1} counterclockwise. The predicted motion along the Philippine Fault near

14°N is 48 mm yr^{-1} towards 280° . This left-lateral motion is the sum of the Legaspi Fault rate (18 mm yr^{-1}) and the Philippine Fault rate south of the junction with the Legaspi (35 mm yr^{-1}). It has a significant thrusting component. The motion along the Verde Passage Fault south of the Macolod Corridor is 40 mm yr^{-1} in a left-lateral sense. The amount of opening deduced within the Macolod Corridor could be close to 40 mm yr^{-1} E–W. The Macolod Corridor in this model thus acts as a left-lateral pull-apart between the Passage Verde Fault and the Philippine Fault, with a component of net extension of about 25 mm yr^{-1} .

In this simple system, the northern part of the Visayas block acts as a cog wheel, allowing the transfer of the Luzon block towards the Manila Trench, the Luzon block being followed by the East Philippine Sliver. It is remarkable that the whole kinematic pattern is such that subduction is everywhere perpendicular to the trenches in spite of the complexities introduced by the collisions of the Benham plateau to the east and the Palawan microcontinent to the west. Although there is a great deal of internal deformation within the Philippine islands outside the major tectonic boundaries that we have used, the velocities involved are so large that this internal deformation appears to correspond only to a minor portion of the whole motion. As a consequence, a simple kinematic description in terms of blocks appears to be quite successful.

7 CONVERGENCE ACROSS THE MOLUCCA SEA

South of the PMB, most of the PH motion is absorbed on both sides of the Molucca Sea (Figs 11 and 12). Elastic loading on the Sangihe subduction zone, to the west of the Molucca Sea, should increase the actual long-term velocity at MANA but elastic loading on the Halmahera subduction zone, to the east of it, should decrease the velocity at TERN. Thus, the two effects should approximately cancel each other out and the convergence of 80 mm yr^{-1} between the two stations should be a good estimate of the long-term subduction within the two trenches. Considering that the PH/SU convergence at this latitude is 105 mm yr^{-1} , the remaining 25 mm yr^{-1} should be absorbed west of the Molucca Sea and also possibly east of TERN, where active deformation is recorded on industrial seismic profiles Pubellier *et al.* (1999).

To the west, south of Mindanao, the Celebes Sea oceanic crust remains apparently undeformed, as indicated by the GPS baseline MANA–ZAMB. No intraplate seismicity is recorded within this marginal basin (Figs 1 and 11) and seismic surveys do not reveal recent deformation of the seafloor (Hinz & Block 1990). However, some active deformation can be observed on industrial seismic profiles along the northwest margin of this basin, offshore of station TAWA in northern Borneo (Figs 5 and 12). In northern Borneo active folding and reverse faulting affect recent sediments known offshore and onshore Brunei (station BRUN discussed in the Introduction). Station TAWA is moving at approximately the same 10 mm yr^{-1} velocity westwards as station BRUN, which indicates that no shortening (less than 5 mm yr^{-1} , taking into account the confidence limits) occurs between the two stations onshore northern Borneo. We conclude that more than 10 and certainly less than 25 mm yr^{-1} of shortening due to the PH/SU convergence is absorbed on both margins of North Borneo. Knowing that 10 mm yr^{-1} is absorbed west of TAWA, the remaining

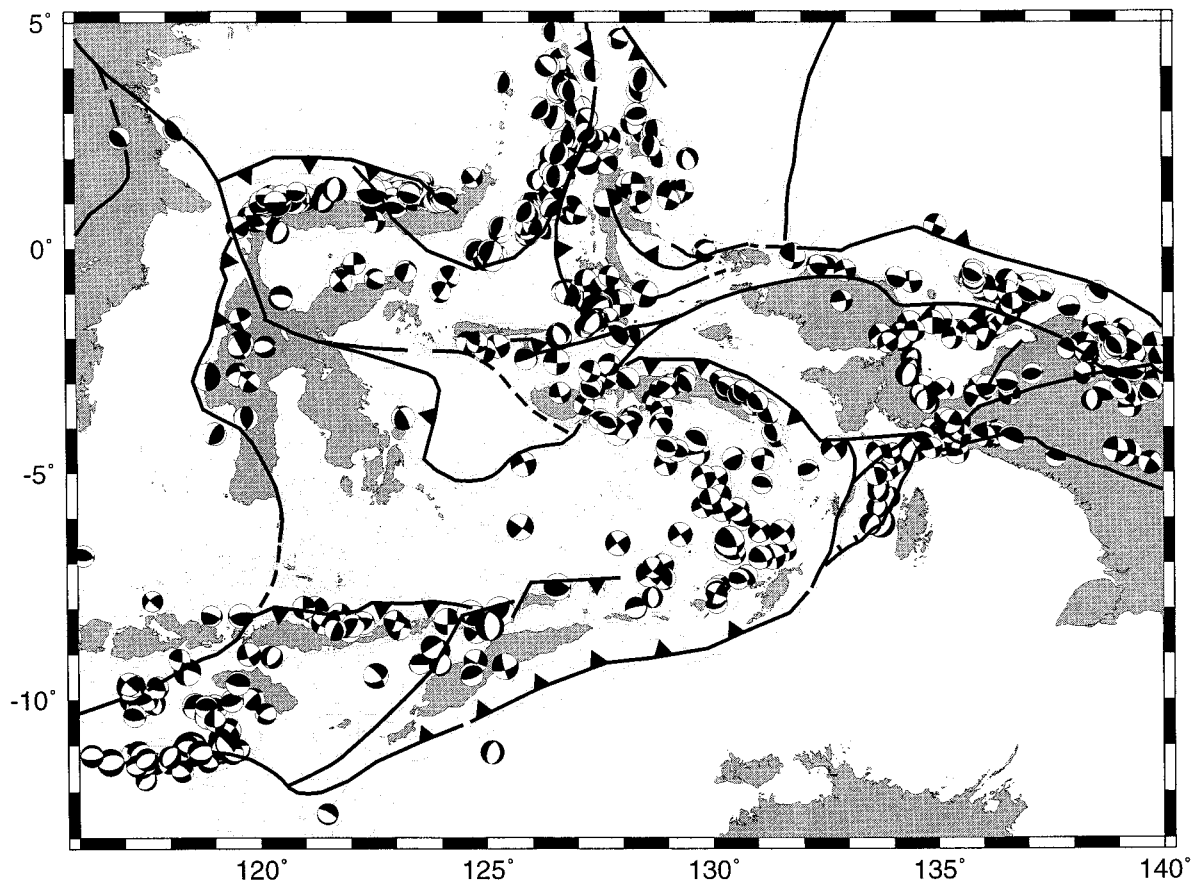


Figure 11. Fault plane solutions around the Banda Sea (Eastern Indonesia): CMT Harvard catalogue, 0–35 km, last 20 yr.

15 mm yr^{-1} should be absorbed on the eastern margin of North Borneo and/or east of TERN. In the absence of an evaluation of the elastic effect at TERN, we cannot split this 15 mm yr^{-1} between the two areas.

8 THE TECTONIC PATTERN AROUND THE TRIPLE JUNCTION AREA

The triple junction of the PH with Sundaland and Australia in the Sulawesi/Banda area is one of the most complex areas in Southeast Asia (Figs 11 and 12). One of the problems which is often addressed when being confronted with a number of large fault zones is knowing which of these are representative in terms of present-day motion at a regional scale. The GEODYSSSEA results provide important constraints on the locations and slip rates of active faults in this area (Walpersdorf *et al.* 1998a). In this paper we estimate the motions on the major active faults and trenches and focus on the qualitative effects of the PH/SU convergence over the deformation of this area. Because the GEODYSSSEA station at BIAK was affected by strong coseismic effects, its results cannot be used, and GEODYSSSEA gives no geodetic information on the north-western part of New Guinea. Puntodewo *et al.* (1994) have reported the results of a set of measurements in New Guinea at SORO, BIAK, SENT, TIMI and WAME, which we will use to cover our gap (Fig. 2). A comparison of their solution at WAME with the GEODYSSSEA solution shows a difference of 7.5 mm yr^{-1} towards 17° , which is probably within the

measurements errors. However, for consistency between the two sets of measurements, we have subtracted this vector from the measurements of the Puntodewo sites (see Fig. 2).

A number of authors (e.g. Genrich *et al.* 1996) have observed that the PH/SU/AU triple junction has not been stable through geological time and that, as a result, the distribution of blocks belonging geologically to the surrounding larger plates does not correspond to the present kinematic pattern. The PH plate boundary has often been traced along the Sorong Fault zone in northern Irian Jaya. This fault connects westwards with the Halmahera Trench. However, the Bird's Head block, to the south of the Sorong Fault, which is a fragment of Australia slivered between the Sorong Fault zone to the north and the Tarera Fault to the south, has been shown by Puntodewo *et al.* (1994) to have a velocity close to that of PH. For example, site SORO has a velocity of only 14 mm yr^{-1} towards 22° with respect to PH (Fig. 3) but 105 mm yr^{-1} towards 255° with respect to AU (Fig. 4). In contrast, site WAME belongs to AU as its velocity with respect to AU is only 4 mm yr^{-1} (Fig. 4). Thus, the Bird's Head block, which is of Australian origin, has been transferred to the PH as Australia moved north, and the southern boundary of PH now lies along the Seram Trough and the Tarera–Paniai fault system.

Neglecting as a first approximation the 10 mm yr^{-1} shortening on both sides of Sabah and in the Meratus range southwards, the SU margin can be traced from the Sangihe Trench (SaT in Fig. 12), connecting southwards along the Kotomobagu/Gorontalo Fault zone (GKFZ in Fig. 12) to the north-verging North Sulawesi Trench (NST in Fig. 12). To the west, the

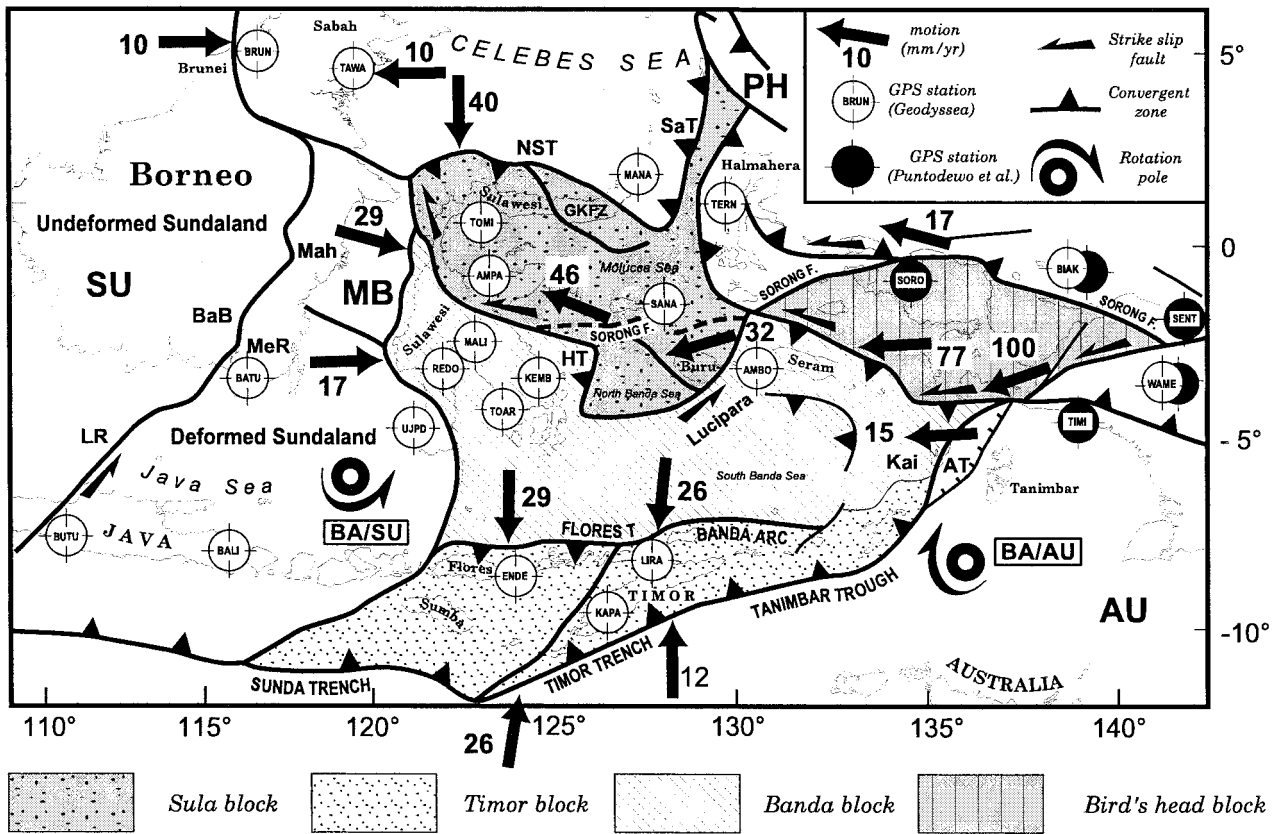


Figure 12. Distribution of the major tectonic boundaries and active mobile microblocks in the PH/SU/AU triple junction. Sundaland (SU), Philippine Sea (PH) and Australia (AU) plates are in white. Microblocks jammed into the triple junction are shown. MB = Meratus Block, Mah = Mahakam, MeR = Meratus Range, GKFZ = Gorontalo-Kotomobaga Fault Zone, SaT = Sangihe Trench, Ht = Hamilton thrust, NST = North Sulawesi Trench, AT = Aru Trough, BA/SU = Banda block rotation pole with respect to Sundaland, BA/AU = Banda block rotation pole with respect to Australia. GEODYSSSEA GPS sites and their acronyms are in white circles and Puntodewo *et al.* (1994) sites in Irian Jaya (SORO, BIAK, TIMI, WAME and SENT) are black. Computed motions across plate boundaries are indicated by black arrows and the corresponding modulus is given in mm yr^{-1} .

tectonic boundary lies east of the Makassar Basin, along the west-verging Sulawesi thrust zone (Bergman 1996). East of station UJPD (Fig. 12), the tectonic boundary is more difficult to trace due to a lack of offshore data.

To the south, the Sunda Trench, offshore Sumatra and Java, extends south of Timor, along the Timor Trench and the Tanimbar Trough (McCauley & Abers 1991, Fig. 12). However, north of the Banda Arc, sites ENDE, KAPA and LIRA move to the north with an azimuth and modulus close to the motion of Australia with respect to SU (Fig. 12). This was previously observed by Genrich *et al.* (1996), who concluded that the Banda arc is now part of Australia. This arc collided with Australia along Timor (Richardson & Blundell 1996) during the Pliocene, at round 5 Ma. However, a small amount of shortening is still absorbed along the easternmost extension of the Sunda Trench, south of Timor, in the Timor Trench and more to the east along the Tanimbar Trough (Milsom *et al.* 1996). This Timor block is thus in the final stage of accretion to the Australian plate. Thus at present, the nascent south-dipping Flores Trench, north of the Banda Arc, accommodates the major part of the Australian convergence and marks the northernmost tectonic front of AU in this area (Fig. 11). The northern limit of the undeformed Australian continent passes into New Guinea island via the extensional Aru Trough (Jongsma *et al.* 1989; Figs 11 and 12), along the left-lateral

Paniai Fault zone (Pubellier *et al.* 1996) and the Irian Jaya frontal thrust (Puntodewo *et al.* 1994).

Between these relatively undeformed large plates, a mosaic of crustal fragments of diverse origins is observed. Here, the boundaries we trace between blocks do not take into account their geological affinities but follow major active faults identified on the basis of the available geological and marine data. The Sula block is the best defined from the active tectonic point of view and its motion is well constrained by the GEODYSSSEA network and data from additional stations (Walpersdorf *et al.* 1998a). It is limited to the north by the North Sulawesi Trench and to the west by the Palu Koro Fault. Its southern boundary is more difficult to trace. A branch could connect with the north-trending Hamilton Thrust (HT in Fig. 12; Silver *et al.* 1983) and another branch with the Sorong Fault zone, west of GPS station SANA. GPS vectors AMPA and SANA indicate a general direction of movement towards the NW, a direction intermediate between the PH and AU directions, at a velocity of about 60 mm yr^{-1} .

Southwards and north of the Flores Trench, the Banda block extends from south Sulawesi and the western South Banda Basin to the west to the Seram Trough and the extensional Aru Trough to the east. The Seram Trough is an active north-verging thrust zone (Linthout *et al.* 1997) connecting to the west with the Lucipara Ridges strike-slip fault

zone (Silver *et al.* 1983) and to the east with the active left-lateral Tarera Fault (Pubellier *et al.* 1998a). The recently opened North Banda oceanic basin (Rehault *et al.* 1991) fills the gap between the Lucipara Fault zone and the Hamilton thrust (Fig. 12). Sites MALI, KEND, REDO, TOAR and AMBO indicate that the Banda (BA) block is undeformed, because these vectors fit a rigid rotation to better than 2 mm yr^{-1} . The rotation pole is situated immediately southeast of site UJPD in southeastern Sulawesi. The rotation rate is $2.65^\circ \text{ Myr}^{-1}$ (see Table 2 and Fig. 12). In Fig. 12, we have identified two additional smaller blocks, the Buru and North Banda Basin blocks, which we consider to be attached to the Sula block.

9 MOTION ALONG THE MAJOR BOUNDARIES WITHIN THE TRIPLE JUNCTION AREA

We will proceed from east to west along first a northern and then a southern section. The northern section, at the latitude of the Bird's Head block, is under the direct influence of PH. The southern one is under the influence of AU. We thus start from the two main plates, PH to the north and AU to the south, and then consider the motions of the blocks intermediate between them and SU. As stated above, the GPS measurements of Puntodewo *et al.* (1994) and McCauley (1996) indicate that the Bird's Head block moves to the west at a velocity close to the PH velocity (Fig. 3): less than 20 mm yr^{-1} of left-lateral motion is absorbed along the Sorong Fault zone (17 mm yr^{-1} towards 233° between BIAK and SORO). 100 mm yr^{-1} towards 250° of left-lateral motion occurs between the Bird's Head block and AU (between SORO and WAME). It follows that a large part of this motion is absorbed along the Tarera and Paniai faults (Pubellier *et al.* 1996, 1998b). However, the Bird's Head block is also affected by strong deformation, between the Sorong and Tarera/Paniai left-lateral faults (Fig. 12). The reader is referred to Puntodewo *et al.* (1994) and McCauley (1996) for a more detailed discussion of the tectonic situation there.

To the west, site SANA, located along a possible westward extension of the Sorong Fault zone, has a motion similar to AMPA that is located on the Sula block. The Buru block thus moves with the Sula block, indicating that the Sorong Fault is not active here, as indicated by the dashed line in Fig. 12. We consequently link the Buru and Sula blocks. The Sorong Fault probably links with a SW-NE fault that forms the southeastern boundary of the Buru block. The differential motion between the Bird's Head block and the Sula/Buru block is 46 mm yr^{-1} towards 280° (SORO/SANA). This is pure convergence absorbed along the southern extension of the Halmahera Trench. As a result, the motion vector in SANA is turned clockwise with respect to SORO (Figs 2 and 11).

The Sula block, which is not a rigid block, has a motion which can be approximated by a clockwise rotation along the curved Palu Fault, with a rotation pole located close to site MANA and a rotation rate of $3.4^\circ \text{ Myr}^{-1}$ (Table 2), as indicated by the results of a local geodetic network linked to GEODYSSSEA (Walpersdorf *et al.* 1998a) and confirmed by geological and palaeomagnetic data (Walpersdorf *et al.* 1998b). The rate of left-lateral strike slip along the Palu Fault is 34 mm yr^{-1} . The geologically recent south-dipping North Sulawesi Trench, pinned to the east near MANA, absorbs the convergence by southward subduction of the Celebes Sea

lithosphere at a rate of 40 mm yr^{-1} at its western extremity, rapidly decreasing eastwards. Thus, the remaining westward PH motion is deflected northwards towards the North Sulawesi subduction.

Moving southwards to the next section, and taking into account the important observation made above that the Banda block, over a total E-W length of more than 1000 km, is undeformed (see Fig. 11), we can derive the relative motions of all blocks with respect to BA, as we have defined precisely the motion of BA/SU using sites AMBO, KEMB, TOAR, REDO and MALI (Figs 2 and 12). The only relative motion that we cannot obtain is the motion of the North Banda Basin, which may be affected by transtension (Rehault *et al.* 1991). The data available in this paper do not give information on the motion of this small block.

The derived BA/AU rotation pole is situated south of the Aru Trough. (Fig. 12). The rate of rotation is $2.35^\circ \text{ Myr}^{-1}$ (Table 2 and Fig. 12). This rotation enables us to compute the motion at the eastern extremity of BA with respect to AU. We first note that the BA/AU pole is situated close to this eastern extremity. Thus BA rotates counterclockwise with respect to AU and its eastern extremity acts as a pivot. Eastern Banda has a motion close to the motion of AU, whereas western Banda moves south with respect to AU. As a consequence, the convergence along the southern boundary of BA progressively decreases towards the east to be transformed into extension within the Aru Trough. The E-W extensional motion predicted there is 15 mm yr^{-1} (Fig. 12). Extensional subsidence within the Aru Trough has been reported by Jongsma *et al.* (1989), and is manifest in the seismicity (Fig. 11).

Moving west, we can obtain for the first time a quantitative estimate of the subduction motion within the Flores Trench, using the BA/AU motion and subtracting the motions of the sites on the Banda and Timor arc. North of LIRA, the motion is 26 mm yr^{-1} towards 183° and north of ENDE, it is 29 mm yr^{-1} towards 171° (Fig. 12). In contrast, the motion along the Timor Trench south of LIRA and KAPA is only 12 mm yr^{-1} towards 190° . It increases to 26 mm yr^{-1} towards 195° south of ENDE (Fig. 4) and then becomes nearly equal to the motion within the Flores Trench. On the western border of BA, the convergence with respect to SU decreases from north (29 mm yr^{-1} towards 277° near 1°S) to south (17 mm yr^{-1} towards 273° near 3.5°S). However, to obtain the actual convergence within the Makassar Straits, one should remove the 10 mm yr^{-1} of E-W convergence absorbed to the west within Borneo. These values then reduce, respectively, to 20 mm yr^{-1} and 9 mm yr^{-1} . Further south, near 5°S , the motion changes to 18 mm yr^{-1} of left-lateral strike-slip to the NW, which reduces to 9 mm yr^{-1} when the western convergence is taken into account. Note, however, that for vectors less than 10 mm yr^{-1} , the error bars of about 5 mm yr^{-1} make the estimation of the orientation of the vector extremely imprecise.

Finally, to the northeast, the motion of 77 mm yr^{-1} towards 91° (using AMBO/SORO) of BA with respect to the Bird's Head block is absorbed along the Seram Trough. This corresponds mostly to left-lateral strike-slip with increasing convergence to the east as the trench curves southwards. The motion between BA and the Buru block of 32 mm yr^{-1} towards 78° (using AMBO/SANA) is absorbed along a left-lateral fault.

From the description above, we can deduce four main conclusions. First, the AU boundary to the west has migrated northwards, with a jump from the Timor Trench to the Flores

Trench, as the plate was moving northwards. Second, to the east, the PH has migrated southwards, from the Sorong Fault to the Tarera and Paniai faults, transferring the Bird's Head block from the Australia plate to the PH as the northward motion of AU was encroaching on PH. Thus, these two plates now have a common boundary to the east. Third, the mosaic of blocks west of the Philippine advancing continental front, the Bird's Head block, is moving northwestwards towards the North Sulawesi Trench, below which the Celebes Sea is being subducted. This escape of blocks away from a collision zone towards the remaining oceanic basins can be compared to the situation within the Eastern Mediterranean. However, here the situation is somewhat different as the collision is oblique and not frontal and the direction of escape of the squeezed mosaic of blocks is necessarily towards the remaining oceanic spaces. Fourth, an undeformed, partly oceanic block (oceanic crust of the South Banda Sea), the Banda block, is rotating with respect to a pivot fixed to AU to the east. The presence of this rigid piece to the south is a strong constraint on the convergence motion and actually results in E–W extension to the east within the Aru Trough. The rotation of BA enables transfer of part of the convergence between AU and SU to the west through subduction of whatever is left of the Makassar Basin.

10 CONCLUSIONS

Our results define the kinematic pattern within a deformed zone along the PH/SU and PH/AU plates boundaries (Fig. 13). In general, there is a good qualitative agreement between the GPS measurements and geological observations. One of the main results is the quantification of overlapping subductions on both sides of the PMB. To the west, convergence decreases from about 90–100 mm yr⁻¹ along the Manila Trench to 50 mm yr⁻¹ NW of Mindoro, north of the zone of collision of Palawan with the PMB. Transfer of 50 per cent of this Manila Trench convergence motion to the Philippine Trench to the east is accommodated principally by rapid counterclockwise rotation of eastern Luzon.

Southwards, convergence decreases regularly along the Philippine Trench from 54 mm yr⁻¹ near 13°N to 32 mm yr⁻¹ east of Mindanao. Inside the PMB, the slip rate of the left-lateral Philippine Fault, which enables complete partitioning to occur at the trench, increases northwards from 22 mm yr⁻¹ at 7°N to 35 mm yr⁻¹ in the Visayas. As a result, the East Philippine Sliver, east of this fault, moves north and transfers this motion to the Luzon block counterclockwise rotation. West of the Philippine Fault, the Visayas block in the central

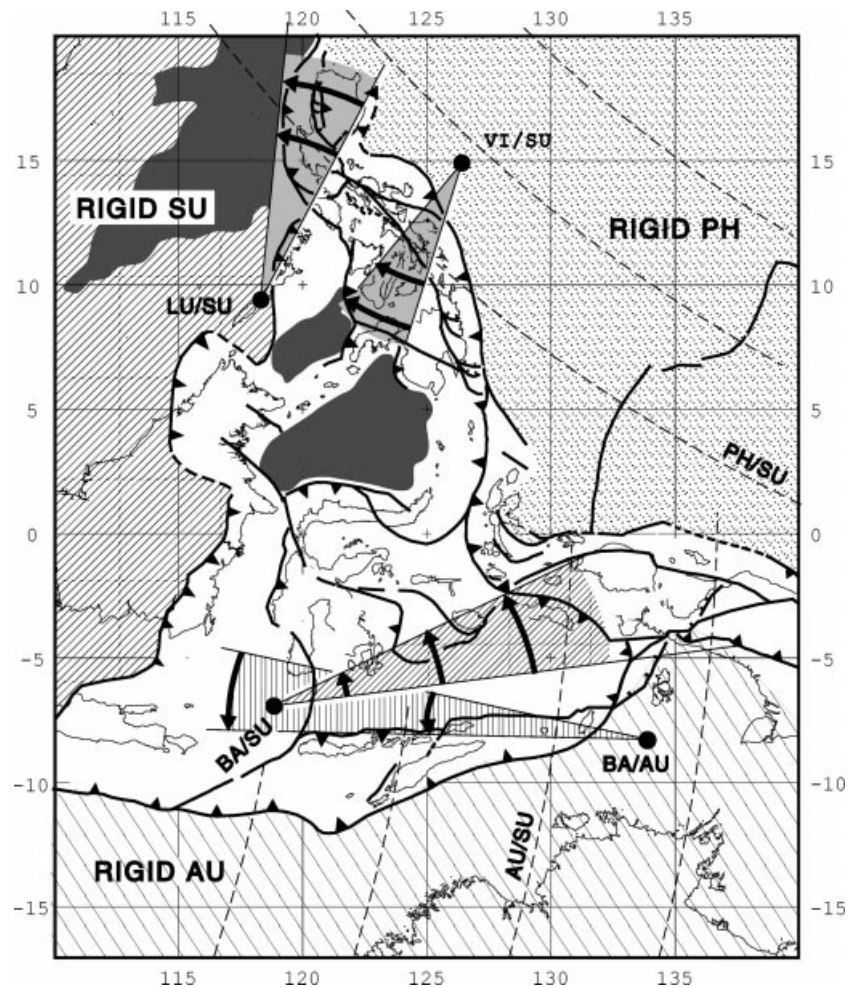


Figure 13. Active tectonics in the Philippines–East Indonesia region: We have differentiated the rigid SU, PH and AU plates (stripes and grey) and the South China Sea, the Sulu Sea and the Celebes Sea oceanic basins (dark grey). Dashed circles represent the rotations of rigid AU and PH with respect to SU. The rotations of the Banda block with respect to SU and AU and of the Visayas and Luzon blocks with respect to SU are also shown. The corresponding rotation poles are shown by solid circles.

Philippines is rotating rapidly clockwise, transferring most of the remaining convergence to the Negros/Cotabato trenches on its western border, up to 32 mm yr^{-1} near 12°N and 50 mm yr^{-1} near 8.5°N . These estimates ignore the amount of convergence absorbed to the west, at the limit of undeformed SU.

The overall scheme of transfer is thus quite simple: two opposing rotations on either side of the left-lateral Philippine Fault, clockwise to the southwest and counterclockwise to the northeast (Fig. 13). As a result, the northern part of the Visayas block acts as a cog wheel with respect to the Luzon block. It is remarkable that this system is such that subduction is everywhere perpendicular to the trenches.

South of Mindanao, within the Molucca Sea, the overlapping divergent subduction system of the PMB is relayed by the convergent Sangihe–Halmahera subduction system. This accommodates 80 mm yr^{-1} of the 105 mm yr^{-1} PH/SU convergence, and about 15 to as much as 20 mm yr^{-1} of the remaining convergence is absorbed far to the west, within the northern Borneo margins.

Deformation in the triple junction area is more difficult to quantify precisely as only a small number of stations are available. However, the presence of a large rigid partly oceanic block, the Banda block, facilitates the evaluation of the kinematics and enables us to quantify the convergence both to the north of the Banda arc, within the Flores Trench, and to the south of it, within the Timor Trench. The Banda block is pinned to the east to AU and rotates clockwise, producing E–W extension to the east within the Aru and Weber troughs. To the west, it transfers part of the AU/SU convergence to eastward subduction of the Makassar Straits. The motions of the blocks between AU, PH and SU is in part governed by the escape towards the remaining oceanic space.

The analysis we have made has confirmed that the kinematics of the Sundaland block found by the GEODYSSSEA programme are compatible with the known relative motions at its tectonic boundaries, whereas the assumption that Sundaland belongs to Eurasia is not compatible with them.

ACKNOWLEDGMENTS

The GPS data used in this paper were acquired within the framework of the GEODYSSSEA project sponsored by the CEE and the ASEAN and led by Peter Wilson. We thank in particular the Mines and Geosciences Bureau in the Philippines and Bakosurtanal in Indonesia for their strong interest in the measurements. We also wish to thank our colleagues of the IFAG (now BKG) and GFZ, both in Germany, for their decisive role in the acquisition of data. We thank Gero Michel, who sent us an important preprint, and Gero Michel, Pierre Henry and two anonymous reviewers for their constructive criticism. We thank S. B. Yu for discussions concerning his GPS data during the latest stage of revision of this paper.

REFERENCES

Bader, A.G., Pubellier, M., Rangin, C. & Deplus, C., 1999. Active slivering of oceanic crust along the Molucca ridge (Indonesia-Philippines). Geodynamic implication, *Tectonics*, in press.
 Barrier, E., Huchon, P. & Aurelio, M., 1991. Philippine fault: a key for Philippines kinematics, *Geology*, **19**, 32–35.

Bergman, S.C., Co eld, D.Q., Talbot, J.P. & Garrard, R., 1996. Tertiary tectonics and magmatic evolution of western Sulawesi and the Makassar strait, Indonesia: evidence for a Miocene continent-continent collision, in *Tectonic Evolution of SE Asia*, eds Hall, R. & Blundell, D., *Geol. Soc. Spec. Publ.*, **106**, 391–429.
 Chamot-Rooke, N., Vigny, C., Rangin, C., Walpersdorf, A., Le Pichon, X. & Huchon, P., 1997. Sundaland motion detected from Geodyssea GPS measurement, part 1: Implications for motion at Sunda trench, *Geodyssea (Geodynamics of the South and Southeast Asia) Concluding Symp.*, Penang, Malaysia, 14–18 April (abstract).
 Chamot-Rooke, N., Le Pichon, X., Rangin, C., Huchon, P., Pubellier, M., Vigny, C. & Walpersdorf, A., 1999. Sundaland motion in a global reference frame detected from GEODYSSSEA GPS measurements—I. Implications for subduction motion along Java, Sumatra and Burma trenches, *Geophys. J. Int.*, in press.
 DeMets, C., Gordon, R.G., Argus, D.F. & Stein, S., 1994. Effect of recent revisions to the geomagnetic reversal time scale on estimates of current plate motions, *Geophys. Res. Lett.*, **21**, 2191–2194.
 Duquesnoy, T., 1997. Contribution de la géodésie à l'étude de grands décrochements actifs associés à des zones de subduction à convergence oblique, Exemple de la grande faille de Sumatra et de la faille Philippine thèse, Université de Paris Sud, Orsay.
 Duquesnoy, T. *et al.*, 1994. Detection of creep along the Philippine Fault: first results of geodetic measurements on Leyte island, central Philippine, *Geophys. Res. Letters*, **21**, 975–978.
 Foster, H., Oles, D., Knittel, U., Defant, M.J. & Torres, R.C., 1990. The Macolod Corridor: a rift crossing the Philippine island arc, *Tectonophysics*, **183**, 265–271.
 Genrich, J.F., Bock, Y., McCarrey, R., Calais, E., Steven, C.W. & Subarya, C., 1996. Accretion of the southern Banda arc to the Australian plate margin determined by GPS measurements, *Tectonics*, **15**, 288–295.
 Hamburger, M., Cardwell, R. & Isacks, B., 1983. Seismotectonics of the Northern Philippines Island Arc, in *Tectonic and Geologic Evolution of Southeast Asian Seas and Islands*, ed. Hayes, D.E., *Am. Geophys. Un. Monogr.*, **27**, 1–22.
 Hamilton, W., 1978. *Tectonics of the Indonesian Region*, USGS Prof. Paper, Washington.
 Heki, K., Miyazaki, S. & Tsuji, H., 1997. Silent fault slip following an interplate earthquake at the Japan Trench, *Nature*, **386**, 595–598.
 Hinz, K. & Block, M., 1990. Summary of the geophysical data from the Sulu and Celebes seas, *Init. Repts Ocean Drilling Program*, **124**, 87–92.
 Hinz, K., Fritsch, J., Kempter, E.H.K., Manaf Mohamad, A., Meyer, J., Mohamed, D., Vosberg, H. & Weber, J., 1989. Thrust tectonics along the north-western continental margin of Sabah/Borneo, *Geol. Rund.*, **78**, 705–730.
 Jongsma, D., Huson, W., Woodside, J.M., Suparka, S., Sumantri, T. & Barber, A.J., 1989. Bathymetry and geophysics of the Snellius II triple junction and tentative seismic stratigraphy and neotectonics of the Northern Aru Trough 1989, *Netherland J. Sea Res.*, **24**, 231–250.
 Karig, D.E., 1973. Plate convergence between the Philippines and the Ryukyu islands, *Mar. Geol.*, **14**, 153–158.
 Kato, T., Kotake, Y., Chachin, T., Iimura, Y., Miyazaki, S., Kanazawa, T. & Suyehiro, K., 1996. An estimate of the Philippine Sea Plate motion derived from the Global Positioning System: observation at Okino Torishima, *Japan. J. Geodetic Soc. Japan*, **42**, 223–243.
 Lallemand, S.E., Popo, M., Cadet, J.-P., Bader, A.-G., Pubellier, M., Rangin, C. & Deontaines, B., 1998. Genetic relations between the central and southern Philippine Trench and the Sangihe Trench, *J. geophys. Res.*, **B103**, 933–950.
 Le Pichon, X., Chamot Rooke, N., Vigny, C., Walpersdorf, A., Huchon, P. & Rangin, C., 1997. Sundaland motion detected from Geodyssea GPS measurement, part II: Relative motion of Sundaland

- and South China blocks, implications on India/Eurasia collision and on the tectonics of Taiwan, *Geodysea (Geodynamics of the South and Southeast Asia) Concluding Symp.*, Penang, Malaysia, 14–18 April (Abstract).
- Le Pichon, X., Mazzotti, S., Henry, P. & Hashimoto, M., 1998. Deformation of Japanese islands and seismic coupling: an interpretation based on GSI permanent GPS observations, *Geophys. J. Int.*, **134**, 501–514.
- Le Rouzic, S. & Gaulon, R., 1997. Seismotectonic analysis of the lineament of Legaspi, (Philippines); seismic crisis of 1995–96, *EOS, Trans. Am. geophys. Un.*, **78**, 718.
- Lewis, S.D. & Hayes, D.E., 1983. A geophysical study of the Manila Trench, Luzon, Philippines; forearc basin structural and stratigraphic evolution, *J. geophys. Res.*, **89**, 9196–9214.
- Linthout, K., Helmers, H. & Sopaheluwakan, J., 1997. Late Miocene obduction and microplate migration around the southern Banda Sea and the closure of the Indonesian Seaway, *Tectonophysics*, **281**, 17–30.
- Marchadier, Y. & Rangin, C., 1989. Passage subduction-collision et tectoniques superposées à l'extrémité de la fosse de Manille (Mindoro-Tablas, Philippines), *C. R. Acad. Sci. Paris*, **302** (II), 1715–1720.
- McCabe, R., Almasco, J. & Diegor, W., 1982. Geologic and paleomagnetic evidence for a possible Miocene collision in western Panay, Central Philippines, *Geology*, **10**, 325–329.
- McCa rey, R., 1996. Slip partitioning at convergent plate boundaries of SE Asia, in *Tectonic Evolution of SE Asia*, eds Hall, R. & Blundel, D., *Geol. Soc. Spec. Publ.*, **106**, 3–18.
- McCa rey, R. & Abers, G.A., 1991. Orogeny in arc-continent collision; the Banda Arc and western New Guinea, *Geology*, **19**, 563–566.
- Michel, G.W. et al., 1998a. GPS and paleoseismological studies in Central and SE Asia: the seismic loading cycle, *AGU Tapei Mtng*, **79**, W12 (abstract).
- Michel, G.W., Angermann, D., Wilson, P., Reigber, C.H. & Klotz, J., 1998b. Transient versus secular motion: the possible impact of earthquakes and interseismic loading on the GEODYSSSEA site motions, in *The Geodynamics of S and SE Asia (GEODYSSSEA) project*, Scientific Technical Report STR/98/14, GFZ, pp. 75–97, Postdam.
- Milsom, J., Kayes, S. & Sardjono, 1996. Extension, collision and curvature in the eastern Banda Arc, in *Tectonic Evolution of SE Asia*, eds Hall, R. & Blundel, D., *Geol. Soc. Spec. Publ.*, **106**, 85–94.
- Miyazaki, S., Saito, T., Sasaki, M., Hatanaka, Y. & Imura, Y., 1997. Expansion of GSI's nationwide GPS array, *Bull. geogr. Surv. Inst.*, **43**, 23–34.
- Nichols, G., Hall, R., Milsom, J., Masson, D., Parson, L., Sikumbang, N., Dwiyanto, B. & Kallagher, H., 1990. The southern termination of the Philippine Trench, *Tectonophysics*, **183**, 289–304.
- Okada, Y., 1992. Internal deformation due to shear and tensile faults in a half space, *Bull. seism. Soc. Am.*, **82**, 1018–1040.
- Pinet, N. & Stephan, J.F., 1990. The Philippine wrench fault system in the Ilocos Foothills, Northwestern Luzon, Philippines, *Tectonophysics*, **183**, 207–224.
- Pubellier, M., Girardeau, G., Permana, H. & De ontaines, B., 1996. Escape tectonics during and after collision in Western Irian Jaya, Indonesia, *EOS, Trans. Am. geophys. Un.*, **77**, 654.
- Pubellier, M., Quebral, R., Aurelio, M. & Rangin, C., 1996. Docking and post-docking tectonics in the southern Philippines, in *Tectonic Evolution of SE Asia*, eds Hall, R. & Blundel, D., *Geol. Soc. Spec. Publ.*, **106**, 511–523.
- Pubellier, M., Girardeau, J. & Tjashuri, I., 1998a. Accretion history of Borneo inferred from the polyphase structural features in the Meratus Mountains, in *Gondwana Dispersion and Asian Accretion—Final Results of IUGS IGCP 321*, pp. 103–115, ed. Metcalfe, I., A. A. Balkema, Rotterdam.
- Pubellier, M., De ontaines, B. & Chorowicz, J., 1998b. Active denudation morphostructures from SAR ERS-1 images (SW Irian Jaya), *Int. J. Rem. Sensing*, **20**, 789–800.
- Pubellier, M., Bader, A.G., De ontaines, B., Rangin, C. & Quebral, R., 1999. Upper plate deformation induced by subduction of large asperities: Molucca Sea and Mindanao (Philippine, Indonesia), *Tectonophysics*, **304**, 345–368.
- Puntodewo, S.S.O. et al., 1994. GPS measurements of crustal deformation within the Pacific–Australia plate boundary zone in Irian Jaya, *Tectonophysics*, **237**, 141–153.
- Quebral, R., Pubellier, M., Rangin, C. & De ontaines, B., 1996. Eastern Mindanao, Philippines; a transition zone from a collision to strike-slip environment, *Tectonics*, **15**, 713–726.
- Rangin, C., Muller, C. & Porth, H., 1989. Neogene geodynamic evolution of the Visayan region, in *On the Geology and Hydrocarbon Prospects of the Visayan Basin, Philippine*, eds Porth, H. & Von Daniels, C.H., *Geol. Jahrbuch*, **B70**, 7–28.
- Rangin, C. et al., 1990a. A simple model for the tectonic evolution of Southeast Asia and Indonesia region for the past 43 m.y., *Bull. Soc. Géol. Fr.*, **8**, VI, **6**, 889–905.
- Rangin, C., Bellon, H., Benard, F., Letouzey, J., Muller, C. & Sanudin, T., 1990b. Neogene arc-continent collision in Sabah, Northern Borneo, *Tectonophysics*, **183**, 305–319.
- Rehault, J.P., Malod, J.A., Larue, M., Burhanuddin, S. & Sarmili, L., 1991. A new sketch of the central North Banda Sea, Eastern Indonesia, *J. SE Asian Earth Sci.*, **6**, 329–334.
- Richardson, A.N. & Blundell, D.J., 1996. Continental collision in the Banda arc, in *Tectonic evolution of SE Asia*, eds Hall, R. & Blundell, D., *Geol. Soc. Spec. Publ.*, **106**, 47–60.
- Ringgenbach, J.C., Pinet, N., Delteil, J. & Stephan, J.F., 1992. Analyse des structures engendrées et régime décrochant par le séisme de Nueva Ecija du 16 juillet 1990, Luzon, Philippines, *Bull. Soc. Géol. France*, **163**, 109–123.
- Ringgenbach, J.C., Stephan, J.F., Pinet, N. & Delteil, J., 1993. Structural variety and tectonic evolution of strike-slip basins related to the Philippine fault system, Northern Luzon, Philippines, *Tectonics*, **12**, 187–204.
- Savage, J.C., 1983. A dislocation model of strain accumulation and release at a subduction zone, *J. geophys. Research*, **88**, 4984–4996.
- Seno, T., Stein, S.A. & Gripp, A.E., 1993. A model for the motion of the Philippine Sea Plate consistent with NUVEL-1 and geological data, *J. geophys. Res.*, **98**, 17941–17948.
- Shell Co., 1996. *Geology and Hydrocarbon Ressources of Negara Brunei Darussalam*, ed. Sandal, S.T., 1996 revision, Brunei.
- Shibutani, T. et al., 1991. Search for the buried subfault(s) of the 16 July 1990 Luzon earthquake, the Philippines, using aftershock observations, *J. Natural Disaster Sci.*, **13**, 29–38.
- Silver, E.A., Reed, D., McCa rey, R. & Joyodiwiryo, Y., 1983. Back-arc thrusting in the in the Eastern Sunda arc, Indonesia, a consequence of arc-continent collision, *J. geophys. Res.*, **88**, 7429–7448.
- Simons, W.J.F. et al., 1999. Plate motions in S.E. Asia: results of the GEODYSSSEA project, *Geophys. Res. Lett.*, in press.
- Walpersdorf, A., Vigny, C., Manurung, P., Subarya, C. & Sutisna, S., 1998a. Determining the Sula block kinematics in the triple junction area in Indonesia by GPS, *Geophys. J. Int.*, **135**, 351–361.
- Walpersdorf, A., Rangin, C. & Vigny, C., 1998b. GPS compared to long-term geologic motion of the north arm of Sulawesi, *Earth planet. Sci. Lett.*, **159**, 47–55.
- Wells, L.D. & Coppersmith, J.K., 1994. New empirical relationships among magnitude, rupture length, rupture width, rupture area, and surface displacement, *Bull. seism. Soc. Am.*, **84**, 974–1002.
- Wilson, P. et al., 1998. Study provides data on active plate tectonics in Southeast Asia region, *EOS, Trans. Am. geophys. Un.*, **79**, 545–549.
- Yu, S.B., Kuo, L.C., Punongbayan, R.S. & Ramos, E.G., 1999. GPS observation of crustal deformation in the Taiwan-Luzon Region, *Geophys. Res. Lett.*, **26**, 923–926.